2011

Timing for hippocampal synaptic plasticity

Thomas K. Fung

Timing for hippocampal synaptic plasticity

(Thesis format: Monograph)

by

Thomas K Fung

Graduate Program in Physiology

A thesis submitted in partial fulfillment of the

requirements for the degree of

Master of Science

The School of Graduate and Postdoctoral Studies

The University of Western Ontario

London, Ontario, Canada

August 2011

THE UNIVERSITY OF WESTERN ONTARIO
THE SCHOOL OF GRADUATE AND POSTDOCTORAL STUDIES

CERTIFICATE OF EXAMINATION

Supervisor	Examiners
Dr. Stan Leung	Dr. John MacDonald
Supervisory Committee	Dr. Michael Jackson
Dr. Lina Dagnino	Dr. Steven Laviolette
Dr. Jonathan Hore	
Dr. Wei-Yang Lu	

The thesis by

Thomas K Fung

Entitled:

Timing for hippocampal synaptic plasticity

Is accepted in partial fulfillment of the
requirements for the degree of
Master of Science

Date

Chair of the Thesis Examination Board

ABSTRACT

The timing of a spike with afferent excitation has been proposed to influence the direction of synaptic plasticity. I hypothesize that positive excitation-spike (ES)-Pairing—generating a synaptic excitation before a spike—results in long-term potentiation (LTP), while the opposite (negative ES-Pairing) results in long-term depression (LTD) *in vivo*. Extracellular potentials were recorded in the hippocampal CA1 region in urethane-anesthetized rats. Basal dendritic excitation was evoked by subthreshold stratum oriens stimulation while stratum radiatum stimulation evoked a spike that invaded the basal dendrites. ES-Pairing (50 times at 5 Hz) at -10, 0 and +10, +20 ES Intervals resulted in a significant potentiation of the slope of the basal excitatory sink for 2 hr compared to controls. Pairing at -20 ms ES Interval did not result in significant potentiation compared to controls. Thus, dendritic excitation occurring within a short time window of a spike results in LTP *in vivo*.

Keywords: long-term potentiation; spike-timing dependent plasticity; hippocampus; basal dendrites; apical dendrites; CA1; rats; current source density; population spike; backpropagation

ACKNOWLEDGEMENTS

I would like to thank everyone who was supportive throughout my academic career. First and foremost, I would like to extend my appreciation and gratitude to my supervisor, Dr. Stan Leung, for the opportunity to develop my knowledge on the basic principles of neuroscience. His patience, guidance, and expertise on electrophysiological methods allowed me to grow as a researcher and a student. Thank you for challenging me to think about things from different perspectives and for providing me with a positive and stimulating atmosphere. I would also like to thank all the members of my lab for their friendship, support, and assistance. Specifically, thanks to Pascal Peloquin for teaching me the skills necessary to start and complete this project and to Min-Ching Kuo for her advice when I needed it most.

I would also like to thank my advisory committee, Dr. Lina Dagnino, Dr. Jonathan Hore, and Dr. Wei-Yang Lu, for reading the draft of my thesis and for providing helpful advice and encouragement throughout the years. Finally, I would like to thank my parents. Their never ending moral support provided me with the focus and motivation to persevere through the difficult times. Thank you to everyone. I would not have been able to do it without all of you.

TABLE OF CONTENTS

LIST OF FIGURES

LIST OF ABBREVIATIONS

-	negative
+	positive
AEP	average evoked potential
AMPA	α-amino-3-hydroxy-5-methyl-4-isoxazole propionic acid
AMPAR	α-amino-3-hydroxy-5-methyl-4-isoxazole propionic acid receptor
ANOVA	analysis of variance
AP	action potential
BAP	backpropagating action potential
CA	cornu ammonis
Ca^{2+}	calcium
CaMKII	calcium/calmodulin(CaM)-dependent protein kinase II
CSD	current source density
D-AP5	D-2-amino-5-phosphoneopentanoic acid
DG	dentate gyrus
EC	entorhinal cortex
EPSP	excitatory postsynaptic potential
ES-Pairing	excitation-spike-Pairing
fEPSP	excitatory field postsynaptic potential
Fig.	figure
IPSP	inhibitory postsynaptic potential
K^+	potassium
LTD	long-term depression
LTP	long-term potentiation
mGluR	metabotropic glutamate receptor
Na^+	sodium
NMDA	N-methyl-D-aspartate
NMDAR	N-methyl-D-aspartate receptor
PBS	primed-burst stimulation
pEPSP	population excitatory postsynaptic potential
PPD	paired-pulse depression
PS	population spike
STDP	spike-timing dependent plasticity
STP	short-term plasticity
VDCCs	voltage-dependent Ca^{2+} channels

1. LITERATURE REVIEW

1.1 Introduction

One of the most important and fascinating properties of the brain is its plasticity. The brain has the capacity to modify neural circuit function and modify thoughts, feelings, and behavior. Synaptic plasticity specifically refers to activity-dependent modification of the strength of synaptic transmission at pre-existing synapses, and has been proposed to play a central role in the capacity of the brain to incorporate experiences into memory. Ever since the introduction of the 'Hebbian' synapse in 1949, which proposed the possibility that memories are the result of small scale changes at neuronal levels (Hebb, 1949), researchers were interested in uncovering the model of synaptic plasticity. One type of synaptic plasticity, long-term potentiation, is a long-lasting increase in synaptic transmission and was first shown in the hippocampus (Bliss and Lomo, 1973). The hippocampus has been implicated in various forms of memory and is one of the most highly studied structures in the investigation of synaptic plasticity.

1.2 The Hippocampus

The hippocampus is a structure within the limbic system. The limbic system, a ring of anatomical structures just rostral to the brainstem, was first defined by J.W. Papez. It commonly includes the hippocampal formation, cingulate cortex, hypothalamus, nucleus accumbens, and amygdala (Isaacson, 1980; Morgane et al., 2005). The hippocampus system plays a role in learning, memory, and visceral and motor responses

involved in defense and reproduction (Van Hoesen, 1995). The hippocampus, which includes the dentate gyrus, appears as in interlocked C-shaped structure with its long axis extending from the rostrodorsal septal nuclei to the caudoventral temporal lobe (Amaral and Witter, 1989).

1.2.1 Anatomy

The hippocampal formation, located on the medial aspect of the temporal lobe, is comprised of four interconnected cortical regions: the hippocampus proper, the dentate gyrus (DG), the subiculum complex (further subdivided into subiculum, presubiculum, and parasubiculum), and the entorhinal cortex (EC) (Amaral and Witter, 1989). In the rodent brain, the hippocampus proper is named cornu ammonis (CA) and is divided into three subregions (CA3, CA2, and CA1) based on their anatomical differences in the cells and the connections (**Fig. 1A**). There are two principal cell types distributed within the hippocampus. Granule cells are the principal cell type of the DG. These cells are located within the stratum granulosum and unlike pyramidal cells, contain a single dendritic branch projecting into the stratum lacunosum-moleculare. Pyramidal cells, which are the principal cell type in the hippocampus proper are layered through the region and are large triangular or ovoid-shaped neurons (Knowles, 1992; Turner et al., 1998).

The hippocampus has a characteristic lamellar structure, with relation to the organization of the cells and their connections. The layers starting from the superficial aspect, are the stratum oriens, stratum pyramidale, stratum radiatum, and stratum

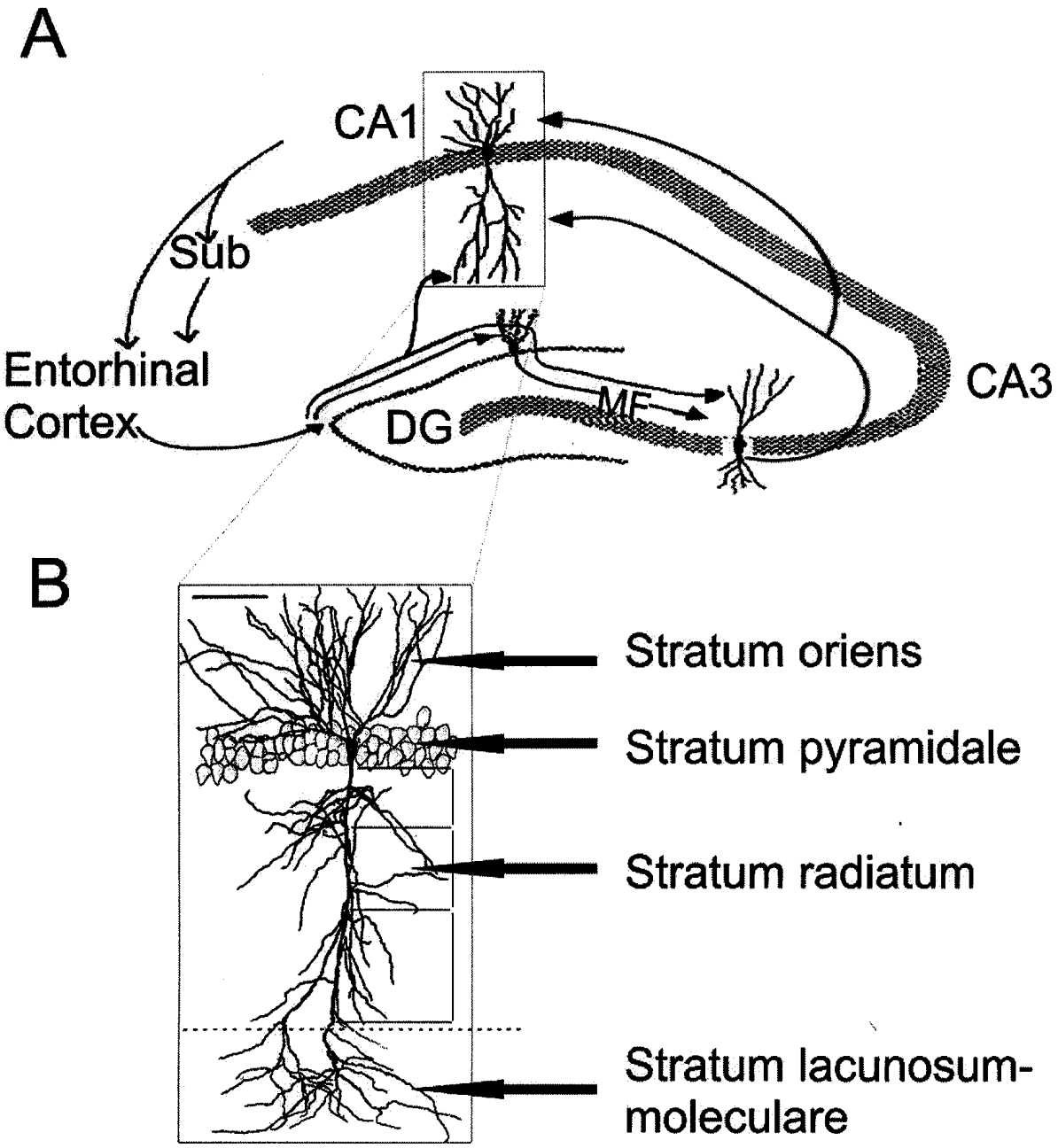

Figure 1. *Schematic diagram of a transverse section through the hippocampal formation, depicting major circuitry and layers.* **A:** The hippocampal formation illustrated with the trisynaptic circuit plus other projections. Arrows indicate the main direction of information propagation. Information enters via the perforant path from the entorhinal cortex and exits via the axons of the CA1 pyramidal neurons. Abbreviations: DG (dentate gyrus), MF (mossy fibers), Sub (subiculum). **B:** Organization of the layers within the CA1 region of the hippocampus (originally illustrated by Megias et al., 2001).

lacunosum-moleculare (**Fig. 1B**). The stratum pyramidale is a dense layer of neuronal cell bodies with dendrites projecting in both directions above and below it. These dendrites of the pyramidal cells in CA3, CA2, and CA1 are called the apical and basal dendrites. The basal dendrites extend to the stratum oriens and the apical dendrites extend into the stratum radiatum and the stratum lacunosum-moleculare (**Fig. 1B**). The apical dendrites can be further broken down into proximal (stratum radiatum) and distal components (stratum lacunosum-moleculare). Although the CA3, CA2, and CA1 region all have pyramidal cells, their cell properties are different. The CA1 pyramidal cell dendrites are shorter than those in CA3. However, they have more homogeneity in their dendritic tree length, while dendritic lengths vary for CA3 pyramidal cells (Ishizuka et al., 1995; Pyapali et al., 1998). Another difference between CA3 and CA1 is that the pyramidal cell layer in CA1 is tightly packed, while it is loosely packed in CA3/CA2. Also, CA2, although similar to the CA3, it is a small region that is less discrete than CA3 and also a matter of some controversy. It is a narrow zone of cells between CA3 and CA1, which have large cell bodies like CA3 but does not receive mossy fiber innervations like CA1.

In addition to the principal cells of the hippocampus, there are a variety of interneurons that play a critical role in regulating excitatory activity all throughout the region. Inhibition of the soma moderates sodium spikes and thus neuronal output, whereas dendritic inhibition, which controls the generation of calcium spikes, is associated with dendritic synaptic plasticity (Megias et al., 2001). Basket cells are located in the pyramidal cell layer. Their dendrites extend into the stratum oriens, the stratum radiatum, and the stratum lacunosum-moleculare. They get excitatory input from

pyramidal cells, but each pyramidal cell contributes only 1 synapse to a particular basket cell. However, the degree of pyramidal cell convergence on an individual basket cell is enormous since basket cell dendritic trees can receive 200 excitatory inputs. The axons of basket cells innervate the soma and the proximal dendrites of the pyramidal cells and can make two to ten synapses on each. From this evidence, there is a huge inhibitory influence of basket cells over a large population of pyramidal cells. There is also inhibitory influence from other interneurons as well. Axo-axonic cells have their cell bodies in the pyramidal cell layer as well. Their dendrites span the entire hippocampal strata. Their axons travel to just below the pyramidal cell layer and terminate on the proximal axons of the pyramidal cells. Each axo-axonic cell terminates on 1200 pyramidal cell axon initial segments and each segment is innervated by 4-10 axo-axonic cells. The cell body and dendritic tree of another type of interneuron, the O-LM (oriens lacunosum-moleculare) are located in the zones occupied by the recurrent pyramidal cell collaterals (Lacaille et al., 1987). In CA3, they are in all strata except the stratum lacunosum-moleculare and in CA1 it is only in stratum oriens. The axons terminate mostly in the distal dendrites of pyramidal cells. The bistratified interneurons have their cell bodies close to the pyramidal cell layer. Axons from these cells are sent to the deep portion of the stratum radiatum and terminate on both the dendritic shafts and spines of pyramidal cells. Their dendrites reside in the zone of associational connections in CA3 and the Schaffer collateral fibers in CA1. Therefore they are driven in a both feedforward and feedback manner. There are more types of interneurons in the hippocampus such as the LM neurons, IS neurons, and the horizontal and radial trilaminar cells. All of these interneurons including the ones talked about in detail are GABAerigic interneurons and

ultimately, their purpose is to balance neuronal excitation with inhibition (Megias et al., 2001).

1.2.2 General Circuitry

The three dimensional circuitry of the hippocampus is complex and unlike the conventional 'lamellar' organization originally proposed (Anderson et al., 1971). Hippocampal projections in the septo-temporal or longitudinal domain are just as prominent as in the transverse plane (Amaral and Witter, 1989; Ishizuka et al., 1990). All the connections in the hippocampus are linked one to the next by largely, but not solely, unidirectional pathway. The classical view is that the EC projects to the hippocampus in a trisynaptic circuit consisting of three synapses. The EC is the first step in the intrinsic circuit and projects to the DG through the perforant path. These principal cells of the DG, granule cells, give rise to axons called mossy fibers that connect to the CA3 pyramidal cells. From there, the CA3 pyramidal cells project to CA1 pyramidal cells via Schaffer collateral axons. The CA1 closes the loop by projecting not only to the subiculum but to the EC as well. The projection ends in the deep layers of the EC in contrast to the beginning of the circuit, which starts in the superficial layers of the EC.

In addition to the trisynaptic loop, there are other connections that deviate from the classical pathway within the hippocampus. For example, the CA3 has associational connections to other regions of the ipsilateral CA3 and also commissural connections that project to the contralateral CA3. Also, information entering the hippocampus from the

EC innervates CA1 and CA3 directly (Amaral and Witter, 1989). The direct projection from EC to CA1 terminates on the distal portion of the CA1 which is close to the subiculum. The direct projection from EC to CA3 projects to the stratum lacunosum-moleculare of the CA3. This projection comes from cells in layer II and collaterals of the same layer II cells reach both the DG and the CA3/CA2, which implies that similar information reaches these structures. All portions of the CA3/CA2 project to CA1 through Schaffer collaterals that innervate both the apical and basal dendrites in the stratum radiatum and stratum oriens respectively (**Fig. 1**). However, CA1 pyramidal cells receive inputs at both apical and basal dendrites from different regions of the CA3: CA3c projects mainly to the apical dendrites, CA3a projects mainly to the basal dendrites, and CA3b projects to both apical and basal dendrites in CA1 (Ishizuka et al., 1990; Li et al., 1994). CA3 gives rise to highly collateralized axons that follow both transverse and oblique orientations through CA1 (Ishizuka et al., 1990). There is a topographical organized network in which certain CA3 cells are more likely to contact certain CA1 cells. It is important to note the unidirectional characteristic of all of these connections compared to the cortex, which contains many bidirectional connections.

1.3 Extracellular Field Potentials

The extracellular space is a conductive medium permitting the flow of ions, and as such can act as a volume conductor. Neuronal activity within specific regions of the brain creates spatial gradients of potential that ultimately result in current flow within the extracellular space. Thus, extracellular field potentials are measurements of the electrical

fields produced by the activity of a single neuron or a group of neurons. Examples of these field potentials include action potentials (APs) along an axon and potentials from a group of neurons within a brain region.

The hippocampus is an ideal structure for the study of field potentials due to the laminar organization of the pyramidal cells and associated afferent and efferent projections. Classified as an open field, the pyramidal cells are characteristically organized into separate strata, with the somata in the cell layer and the dendrites projecting into adjacent layers. An evoked field potential can be generated via artificial electrical stimulation of afferents to a region following a single pulse stimulation of axons that synapse on the dendrites (**Fig. 2**). As such, the characteristic dipole is the result of local current flowing into the dendrite at the point of activation (sink) and current exiting at distant location (source). In order to maintain electrical neutrality within the intracellular and extracellular medium, current flows in closed circuits forming a dipole field. In effect, the field generated by excitatory post-synaptic potentials (EPSPs) at a population of dendrites is referred to as the population EPSP (pEPSP). If the pEPSPs are sufficiently strong, APs may be generated resulting in a field called the population spike (PS). Furthermore, after this initial excitation, there is a late dendritic negative wave which is thought to result from inhibitory postsynaptic potentials (extracellular IPSP; Leung 1979).

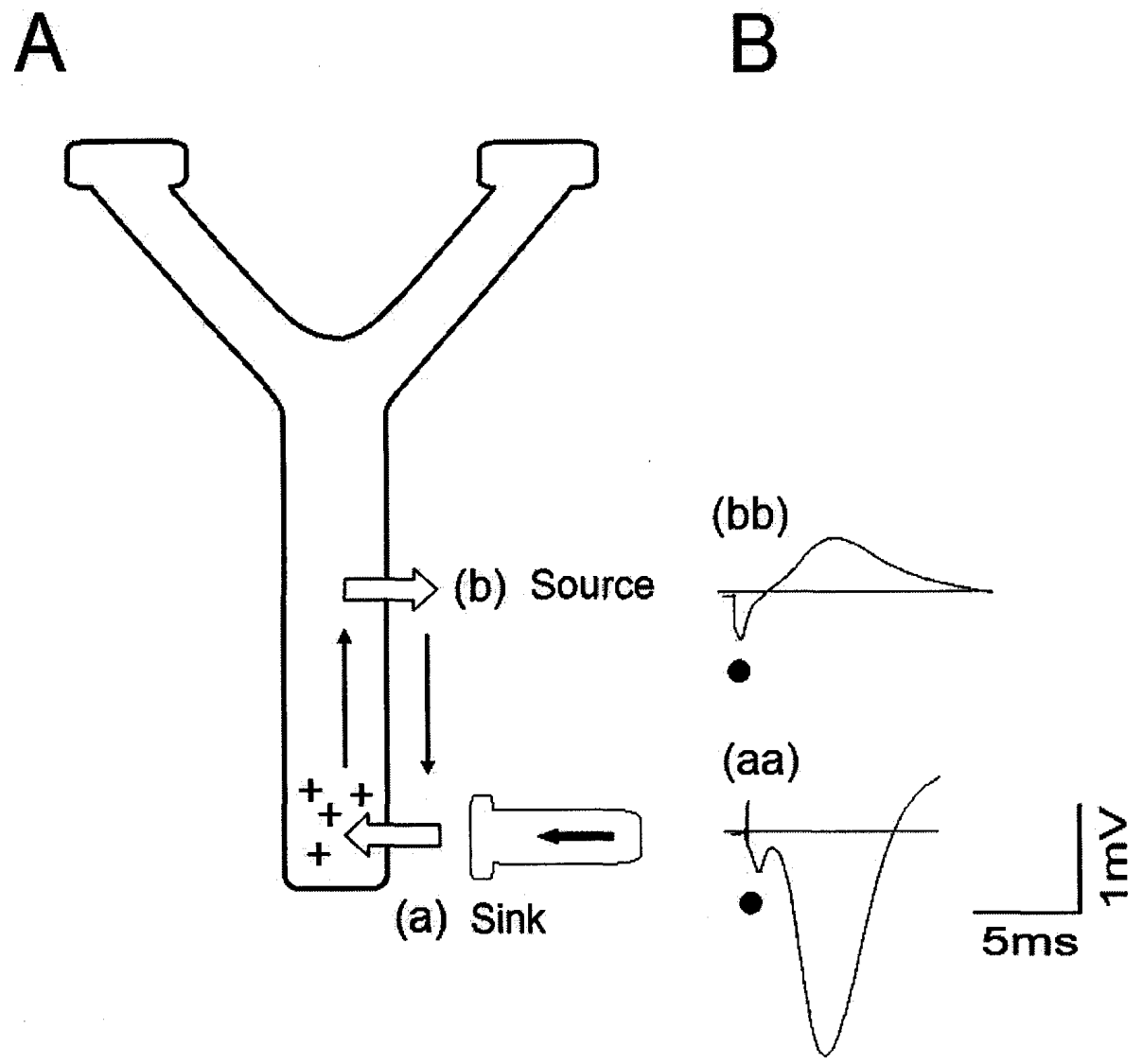

Figure 2. *Schematic diagram of a neuron depicting how current flow through the extracellular and intracellular medium produces characteristic evoked potential profile.* **A:** A simple schematic of a pyramidal cell. Activation of excitatory afferents synapsing on the dendrites results in current flowing in at the point of activation forming a sink (a), flowing intracellularly to a distant location, and finally exiting creating a current source (b). **B:** Current flows in a closed circuit and forms a dipole field, seen as a population EPSP. A 16-channel recording electrode recorded potential flow resembling (aa) and (bb) at sites (a) and (b) respectively. The filled circle indicates the shock artifact.

1.4 Synaptic Plasticity

1.4.1 Long-term Potentiation

The hippocampus was the first structure shown to undergo long-term potentiation (LTP) (Bliss and Lomo, 1973). LTP is a long-lasting increase in synaptic transmission that has been suggested as a cellular mechanism for memory storage (Malenka and Bear, 2004). Early research suggested that LTP is triggered by activation of N-methyl-D-aspartate (NMDA) receptors (NMDARs) (Collingridge et al., 1983). They showed that a specific antagonist of the NMDA subtype of glutamate, D-2-amino-5-phosphoneopentanoic acid (D-AP5), blocks the induction of LTP in area CA1 of the hippocampus. Gary Lynch (1983) further showed that the postsynaptic cell is important in the induction process and established an essential role for calcium by injecting a calcium chelator into CA1 pyramidal cells and finding that it blocked the induction of LTP.

During normal excitatory transmission, glutamate is released from the presynaptic vesicles and binds to and activates α-amino-3-hydroxy-5-methyl-4-isoxazole propionic acid (AMPA) receptors (AMPARs) — ionotropic glutamate receptors that allow movement of monovalent cations such as Na^+ and K^+ through its channel — on the postsynaptic membrane (**Fig. 3; left panel**) (Augustine et al., 2007). Glutamate also binds to the NMDARs but they may contribute little to the excitatory postsynaptic current at rest. However, they are important for synaptic plasticity. At resting membrane potentials, the channels of the NMDARs are blocked by Mg^{2+} (**Fig. 3; left panel**). However, if there is a substantial depolarization, the Mg^{2+} will dissociate and allow for the flow of Na^+ and

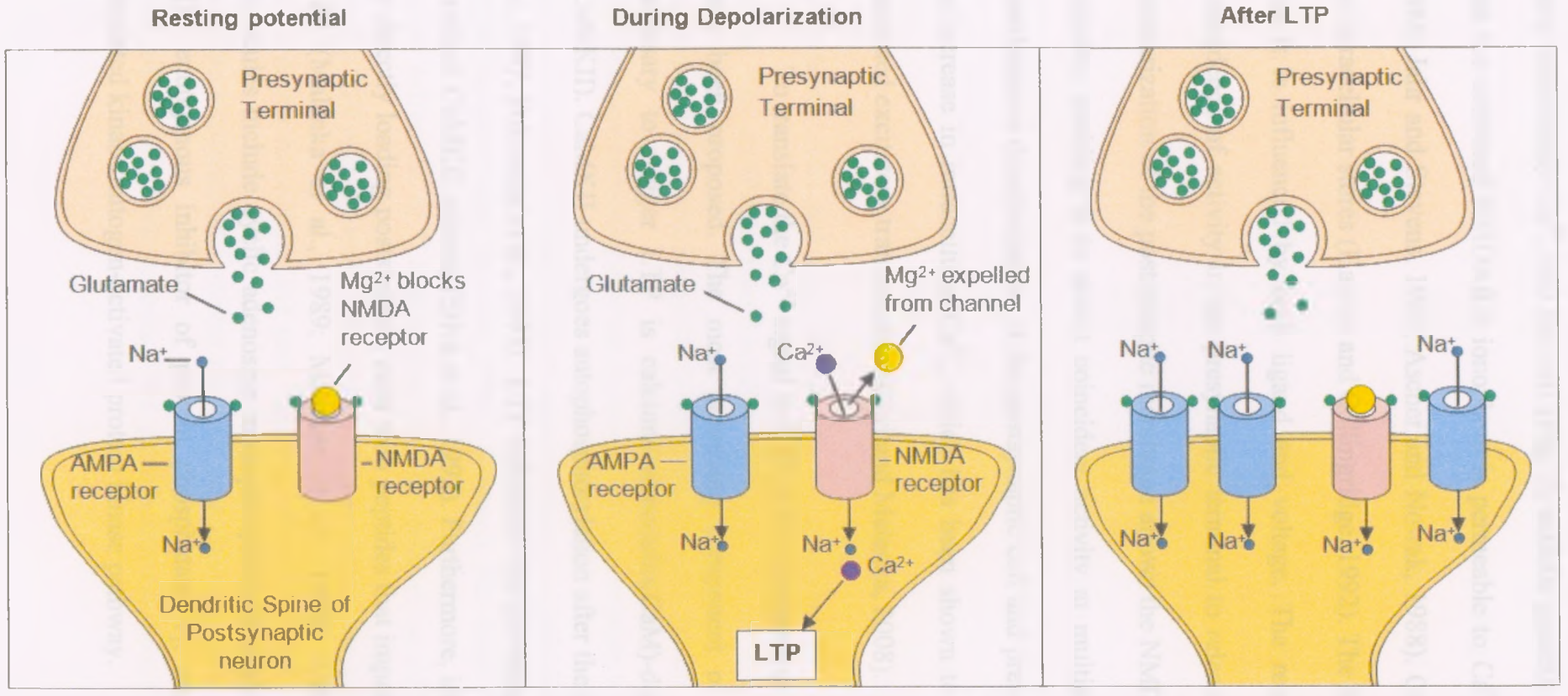

Figure 3. *Schematic diagram depicting the proposed mechanism of LTP.* **Left panel:** Excitation releases glutamate from the presynaptic terminal, which binds to both α-amino-3-hydroxy-5-methyl-4-isoxazole propionic acid (AMPA) and N-methyl-D-aspartate (NMDA) receptors. However, during resting potential, NMDA receptors are blocked by Mg^{2+}. **Middle panel:** During depolarization of the postsynaptic neuron, Mg^{2+} is released and the coincident binding of glutamate allows Na^{+} and Ca^{2+} to enter into the neuron. The influx of Ca^{2+} leads to long-term potentiation (LTP). **Right panel**: A proposed mechanism of LTP after induction. The increase in intracellular Ca^{2+} leads to incorporation of AMPA receptors in the postsynaptic membrane which allows for a larger excitatory response, thus resulting in LTP.

most importantly Ca^{2+} into the cell (**Fig. 3; middle panel**). Several groups have found that the activated NMDAR's ionophore is permeable to Ca^{2+} ions (MacDermott et al., 1986; Jahr and Stevens, 1987; Ascher and Nowak, 1988). Calcium can also be released by intracellular stores (Harvey and Collingridge, 1992). The NMDA receptor is unique in that it is influenced by both ligand and voltage. The requirement for the temporal coincidence of activity in the presynaptic terminal to release transmitter plus adequate depolarization of the postsynaptic membrane allows the NMDAR to act as a coincidence detector, enabling it to detect coincident activity at multiple excitatory inputs. Thus, simultaneous depolarization of the postsynaptic cell and presynaptic activation results in an increase in intracellular Ca^{2+}, which has been shown to be the trigger for LTP or increased excitatory transmission (Citri and Malenka, 2008).

To translate the Ca^{2+} signal to LTP, a few prospective key transduction molecules have been proposed. The most promising component of the molecular machinery necessary to trigger LTP is calcium/calmodulin(CaM)-dependent protein kinase II (CaMKII). CaMKII undergoes autophosphorylation after the triggering of LTP (Barria et al., 1997; Fukunaga et al., 1995). LTP induction was prevented in knockout mice lacking a critical CaMKII subunit (Silva et al., 1992). Furthermore, inhibition of CaMKII activity by directly loading postsynaptic cells with peptides that impair CaMKII function blocked LTP (Malenka et al., 1989; Malinow et al., 1989). Other suggested transduction molecules include cyclic adenosine monophosphate-dependent protein kinase, inhibitor 1[an endogenous inhibitor of protein phosphatase 1], and the extracellular signal-regulated kinase/mitogen-activated protein kinase pathway.

Although the exact signal transduction molecules responsible for the induction of LTP remain unknown, there is a better understanding of the major mechanism of expression of LTP due to research in the hippocampal CA1 region. There is evidence that the induction of LTP involves increasing the number of AMPARs in the postsynaptic plasma membrane, driven through activity dependent changes in AMPAR trafficking (Bredt and Nicoll, 2003; Derkach et al., 2007; Malenka and Nicoll, 1999; Malinow and Malenka, 2002; Song and Huganir, 2002). Activation of intracellular signaling cascades and protein kinases (like CaMKII) leads to the addition of AMPARs into the postsynaptic membrane, which results in the expression of LTP (Malenka and Bear, 2004) (**Fig. 3; right panel**). Specifically, during LTP, recycling endosomes in the dendrites containing reserve pool of AMPARs are mobilized and the AMPARs are exocytosed at the perisynaptic sites and not inserted into the postsynaptic density directly (Park et al., 2004). The AMPARs then laterally diffuse in the plasma membrane and are finally trapped and rendered immobile in the post synaptic density via "slot proteins" such as membrane-associated guanylate kinases. LTP also appears to involve a phosphorylation-driven increase in single-channel conductance of AMPARs themselves (Benke et al., 1998; Soderling and Derkach, 2000). However, the detailed molecular mechanism by which activation of CAMKII leads to the increase in AMPARs on the postsynaptic density still remains to be determined. To summarize, simultaneous depolarization of the postsynaptic membrane and presynaptic glutamate release results in a large NMDAR-dependent increase in dendritic spine calcium concentration, which leads to activation of intracellular signaling cascades and protein kinases (like CaMKII). This leads to the

incorporation of additional AMPARs into the postsynaptic density and ultimately results in LTP.

1.4.2 Induction of LTP

Synaptic potentiation is referred to as LTP if the potentiated response is maintained without any downward drift for longer than 30-60 minutes. This is referred to as the early phase of LTP, which is protein synthesis independent (Frey et al., 1993). In addition, there are two other phases: Short term potentiation (STP), which is potentiation that decays to baseline within 30 to 60 minutes and Late LTP, which is a persistent, protein synthesis dependent phase of LTP that occurs after early LTP and can last for hours to days. The LTP that is referred to throughout this paper is LTP of 1-2 h duration, likely corresponding to early LTP of Frey et al.

The most commonly used protocol to induce LTP is a single train of pulses at 100 Hz for 1 second. However, the stimulus patterns used to elicit LTP have varied widely, ranging from brief trains at 400 Hz (Douglas and Goddard, 1975) to single stimuli of high intensity repeated at 1 Hz (Abraham et al., 1986). LTP can also be induced by a widely used technique called primed-burst stimulation (PBS) *in vitro* (Davies et al., 1991). This features a 200 ms interval between a priming stimulus and a brief burst of stimuli (Larson and Lynch, 1986). The priming induction protocol involves a single stimulus that precedes a brief high-frequency burst. The burst contains 2-10 shocks that are at stimulus strengths below threshold for spike firing (Diamond et al., 1988; Larson and Lynch,

1986; Rose and Dunwiddle, 1986). The priming stimulus causes a reduction in the GABA mediated IPSP through activation of feedforward GABA interneurons that leads to $GABA_A$- and $GABA_B$- mediated hyperpolarization in the pyramidal cell (Davies et al., 1991). In addition, some of the GABA that is released as a result of the priming stimulus feeds back to activate $GABA_B$ autoreceptors, which inhibits further GABA release that is maximal at around 100 to 200 ms. So, the priming stimulus releases a normal amount of GABA, but the stimuli during the burst release less GABA, which allows for synaptic activation of NMDARs and enhance the NMDAR-mediated current on pyramidal neurons. The primed burst stimulus, if used minimally, are far more physiologically relevant and more likely to occur naturally than longer trains of hundreds of stimuli like the commonly used 100 Hz for 1 second tetanus. Hippocampal pyramidal neurons can and do fire in high-frequency bursts, but less is known whether LTP can be induced by naturally occurring patterns of activity in freely moving animals *in vivo* (Buzsaki et al., 1987).

LTP can also be induced by a low-frequency pairing or "spike timing" of presynaptic and postsynaptic APs *in vitro* (Bi and Poo, 1998; Buchanan and Mellor, 2007; Montgomery et al., 2001). During spike timing, single pulse afferent stimuli are paired with a depolarizing pulse that fires the cell only once. The timing of the pre- and postsynaptic firing is controlled. LTP is induced if repetitive presynaptic stimulation generates a synaptic response within a 20 ms time window prior to the depolarization of the postsynaptic dendrite (Bi and Poo, 1998; Dan and Poo, 2006; Markram et al., 1997). The reverse, repetitive postsynaptic spiking within a 20 ms time window prior to presynaptic activation induces long-term depression (LTD), a long lasting decrease in

synaptic transmission. This form of synaptic plasticity is known as Spike-Timing Dependent Plasticity (STDP) (Abbott and Nelson, 2000).

1.4.3 Spike-Timing Dependent Plasticity (STDP)

Hebb stated that "when an axon of cell A is near enough to excite a cell B and repeatedly or persistently takes part in firing it, some growth process or metabolic change takes place in one or both cells such that A's efficiency, as one of the cells firing B, is increased" (Hebb, 1949). His statement can be extended to imply that an increase in synaptic weight only occurs when the presynaptic cell fires shortly before the postsynaptic cell. LTP and LTD induction requires a temporal order of stimulation of weak and strong inputs. The earliest experiment on associative LTP used weak and strong inputs (Levy and Steward, 1983). They found that potentiation was produced when the weak input preceded the strong input by less than 20 ms, and reversing the order led to depression in the DG via stimulations of the EC. Later studies further demonstrated the importance of the temporal order of pre- and postsynaptic spiking, revealing a strict critical window of tens of milliseconds (Bi and Poo, 1998; Debanne et al., 1998; Magee and Johnston, 1997; Markram et al., 1997). This form of synaptic plasticity known as STDP (Abbott and Nelson, 2000) has been observed in excitatory synapses in many neural circuits (Boettiger and Doupe, 2001; Cassenaer and Laurent, 2007; Egger et al., 1999; Fieldman, 2000; Froemke and Dan, 2002; Sjostrom et al., 2001; Tzounopoulos et al., 2004). According to Hebb, it is the coincidence, within a narrow time window of firing in the presynaptic cell with sufficient depolarization in the postsynaptic cell that is

the criterion for the induction of LTP. STDP follows this rule and determines the direction of synaptic modification which Hebb implied.

The NMDAR is the coincidence detector: the presynaptic activation provides the glutamate and the postsynaptic depolarization removes the Mg^{2+} block (Mayer et al., 1984; Nowak et al., 1984). The depolarization to remove the block is essential. One method of achieving this depolarization is through backpropagating APs (BAPs). These are APs that are generated in pyramidal cell bodies that propagate back into the dendritic tree. This discovery identified an associative signal at the synapse that could link presynaptic and postsynaptic firing. In hippocampal slice *in vitro* (Magee and Johnston, 1997), a BAP was shown to increase postsynaptic depolarization, Ca^{2+} influx and facilitate LTP. Many of the STDP studies *in vitro* began to use the BAP as the method of postsynaptic depolarization. Once the BAP depolarizes the postsynaptic cell, the Mg^{2+} block is removed and allows for the influx of Ca^{2+}. The amount of Ca^{2+} influx is determined by the induction protocol and determines the direction of synaptic plasticity: high-frequency stimulation leads to fast and large Ca^{2+} influx, whereas low-frequency stimulation leads to prolonged, modest Ca^{2+} rise (Malenka and Bear, 2004; Yang et al., 1999). STDP LTP and LTD also depend on NMDAR activation and the rise in postsynaptic Ca^{2+} levels (Bi and Poo, 1998; Debanne et al., 1998; Feldman, 2000; Magee and Johnston, 1997; Markram et al., 1997; Sjostrom et al., 2001; Zhang et al., 1998).

Induction of STDP LTP requires activation of the presynaptic input milliseconds before the BAP in the postsynaptic dendrite (Caporale and Dan, 2008). The BAP releases the Mg^{2+} and allows for the Ca^{2+} influx leading to LTP induction. The binding of

glutamate to the NMDA receptor occurs for hundreds of milliseconds before it dissociates (Lester et al., 1990), but the STDP LTP window is much shorter than that. The short duration of the window may be due to the kinetics of Mg^{2+} unblocking NMDARs – only depolarization of the postsynaptic neuron from a BAP that occurs soon after the onset of the EPSP can open the NMDARs (Kampa et al., 2004). In addition to the Mg^{2+} unblock of NMDARs, the STDP LTP window can be influenced by interactions between the EPSP and the BAP. For example, the EPSP can affect the dendritic conductance that affect AP backpropagation into the dendrites. In the distal dendrites of CA1 pyramidal neurons, an EPSP that depolarizes the dendrites can inactivate A-type K^+ channels, which regulate the BAP amplitude (Hoffman et al., 1997), and can boost the BAPs arriving within tens of milliseconds (Magee and Johnston, 1997; Watanabe et al., 2002). The boost of the BAP can increase the Ca^{2+} influx through voltage-dependent Ca^{2+} channels (VDCCs), which can modulate the magnitude of the STDP LTP (Bi and Poo, 1998; Froemke et al., 2006; Magee and Johnston, 1997).

The second form of STDP, spike timing dependent LTD, occurs when the order of presynaptic and postsynaptic stimulation is reversed with a time window of 20 ms (Bi and Poo, 1998; Dan and Poo, 2006; Markram et al., 1997). The time window of STDP LTD also depends on Ca^{2+}. Like STDP LTP, there also could be an interaction between the EPSP and the BAP. The BAP creates an afterdepolarization that lasts for tens of milliseconds and an EPSP that coincides with this afterdepolarization leads to a moderate Ca^{2+} influx resulting in LTD. Another proposed model of STDP LTD based on the Ca^{2+} hypothesis (Froemke et al., 2005) suggests that the BAP occurring before an EPSP induces voltage-dependent Ca^{2+} channel dependent Ca^{2+} influx, which inactivates the

NMDARs (Rosenmund et al., 1995; Tong et al., 1995). Inactivated NMDARs results in less Ca^{2+} influx through them and in turn leads to LTD. This model is based on the observations that STDP LTD requires activation of VDCCs (Bender et al., 2006; Bi and Poo, 1998; Froemke et al., 2005; Nevian and Sakmann, 2006) and that EPSP-spike pairing at negative intervals leads to sublinear summation of Ca^{2+} influx (Koester and Sakmann, 1998; Nevian and Sakmann, 2004).

Most of the early experiments on STDP were conducted in slices and cell cultures. These experiments used an *in vitro* model involving intracellular whole cell patch clamping and current injection to depolarize single postsynaptic neurons. A major limitation of these studies was that the nervous system was severed. The trisynaptic circuit was small or absent in the hippocampal slice preparation. Neuronal circuits *in vivo* are much more complex. There are both spontaneous activity and sensory-evoked responses. Barrages of excitatory and inhibitory inputs to neurons may cause the backpropagation of the APs to be more variable *in vivo* (Destexhe et al., 2003). One study showed that spontaneous activity can boost AP backpropagation *in vivo* (Waters and Helmchen, 2004). Also, spontaneous activity can affect membrane potential, conductance, and intracellular Ca^{2+} levels. Zhou et al. (2003) showed that spontaneous postsynaptic spiking makes it more difficult for synaptic potentiation and depression to occur. These factors could complicate the rules for STDP *in vivo*.

1.5 Rationale, Aims, and Hypothesis

Pyramidal cells in the CA1 region of the hippocampus receive inputs at both the apical and basal dendrites; the inputs come from different sets of CA3 neurons (Amaral and Witter, 1989). Stimulation of stratum radiatum excites the apical dendrites of a population of CA1 pyramidal cells that fire a PS. Extracellular mapping showed that the PS evoked by stratum radiatum stimulation originated at the apical dendrites and propagated into the basal dendrites (See Results **Fig. 8**) (Kloosterman et al., 2001). Basal dendritic excitation evoked the reverse PS propagation pattern, originating at the basal dendrites and propagating into the apical dendrites (See Results **Fig. 16**) (Kloosterman et al., 2001). A spike that backpropagates into the dendrites provides a large depolarization that is ideal for unblocking the channels in the NMDA receptors (**Fig. 3B**), and if this depolarization is coincident with afferent (presynaptic) stimulation, LTP would result (Markram et al., 1997). Backpropagated spikes can also be given prior to or after afferent stimulation to test the spike-timing dependent properties of LTP and LTD.

Traditionally, the STDP protocol *in vitro* consists of timing a BAP in the dendrites with low intensity afferent excitation. The BAP results from an AP that is generated in the soma and propagates backwards into the dendrites. This is usually done by voltage clamping patched neurons and giving a strong depolarization in the soma. The afferent stimulation can be done with a stimulating electrode near the dendrites that receive the pairing. Both the presynaptic and postsynaptic depolarizations are performed on cultured hippocampal preparations and acute hippocampal slices. The advantage of this type of protocol is that it allows for precise control of the timing between presynaptic

and postsynaptic depolarization. This method also allows for precise selection of the pathway between two neurons in the hippocampus. However, the main disadvantage is that cultured hippocampal preparations and hippocampal slices deviate from the physiological conditions in an intact hippocampal network. A hippocampal slice preparation only has intact connections in the plane of the section – connections that run outside the sectioned slice are disconnected.

The technique in this study offers an advantage from *in vitro* experiments in that it is performed under actual physiological conditions and not just '*in vivo* like' conditions. This allows for the testing of predictions of pre- and postsynaptic STDP models that have been put forth to explain the timing dependence of LTP and LTD. Another difference is the study of STDP in the CA1 basal dendrites rather than the apical dendrites. This will give insight to the synaptic plasticity properties of the less commonly studied dendritic tree of CA1 pyramidal neurons. This study also uses a modified form of the backpropagated spike. Not only does this experiment study a population of neurons compared to a single neuron, it uses a dendritic PS that originates from the opposite dendrite, propagates past the cell body and invades into the adjacent dendrite. A high intensity synaptic excitation is needed for this and differs from *in vitro* BAPs, which are generated by depolarizing the cell body. Using a protocol that more closely resembles physiological conditions *in vivo* could complicate the rules for synaptic plasticity, but would further the understanding of the mechanisms behind STDP.

The present project will study whether pairing dendritic excitation with a backpropagated PS in CA1 region can induce LTP in the hippocampus. An excitatory

afferent stimulation given to the basal dendrites will be paired with a spike backpropagated from the apical dendrites. My first hypothesis is that at a particular dendrite (basal or apical), coincidence of its excitatory synaptic input with a backpropagated spike gives the optimal condition for LTP *in vivo*. There is also a discrete time window, or excitation-spike (ES) Interval, in the STDP protocol in which LTP or LTD will be induced. So, my second hypothesis is that LTP is induced when presynaptic excitation occurs before the postsynaptic spike (positive ES-Pairing), whereas LTD is induced when the postsynaptic spike occurs before presynaptic excitation (negative ES-Pairing) in the CA1 basal dendrites *in vivo*.

2. METHODOLOGY

2.1 Animals

Adult male Long-Evans rats, weighing between 250g and 400g, were used. Rats were housed in standard cages in a temperature-regulated environment in a 12:12h light/dark cycle commencing at 7 am. Animals had ad-lib access to food and water. Experiments were conducted during the day (10 am – 7 pm). Prior to the commencement of the surgery, rats were housed in the animal headquarters for a minimum of 3 days.

2.2 Electrode implantation

2.2.1 Electrodes

Stimulating electrodes were constructed out of stainless steel wire, 0.005 inches in diameter, insulated with Teflon except at the tips. These electrodes were used for stimulation only. Silicon recording probes were purchased from NeuroNexus, Ann Arbor, MI. The probes had 16 recording sites spaced 50 or 100 μm apart on a vertical shank (Model #: a1x16-5mm50-177).

2.2.2 Surgery

Rats were anesthetized with 30% urethane anesthesia (1.5g/kg solution i.p.). Following urethane administration, atropine methyl nitrate (0.1 ml of 0.5 mg/ml solution

i.p.) was administered in order to block excess salivation. The animals were secured in a stereotaxic frame, the skull surface was exposed and oriented such that lambda and bregma were in a horizontal plane, and burr holes were drilled to prepare for implantation. Two stimulating electrodes were lowered into CA3a/b of the hippocampus respectively. Electrodes were fixed at the coordinates (P3.2, L2.2) and (P3.2, L3.2) relative to bregma (Paxinos and Watson, 1986). The 16-channel recording electrode was lowered into the CA1 region of the hippocampus at the coordinate (P3.8, L1.8). The exact electrode depth varied between animals and so the location was based upon the profile of the evoked potentials monitored during electrode implantation. The recording electrode was lowered to a depth of ~3.5 mm to record from both the basal and apical dendrites of the CA1 pyramidal cells (**Fig. 4**). The CA3a electrode was lowered to a depth of ~3.5 mm into the stratum radiatum to activate the CA1 apical dendrites and the CA3b electrode was lowered to a depth of ~3.0 mm into the stratum oriens to activate the CA1 basal dendrites (**Fig. 4**). The ventral coordinates were calculated relative to the skull surface. Based on established electrophysiological criteria (Leung, 1979), the final depths of the electrodes were optimized by their responses to cathodal stimulation of the deep electrode. Finally, two screws were secured on the skull surface above the frontal cortex and at the cerebellum to serve as stimulus ground and recording ground, respectively. After the surgical preparation, a 1-2 h intermission was given before recording in order to optimize the response.

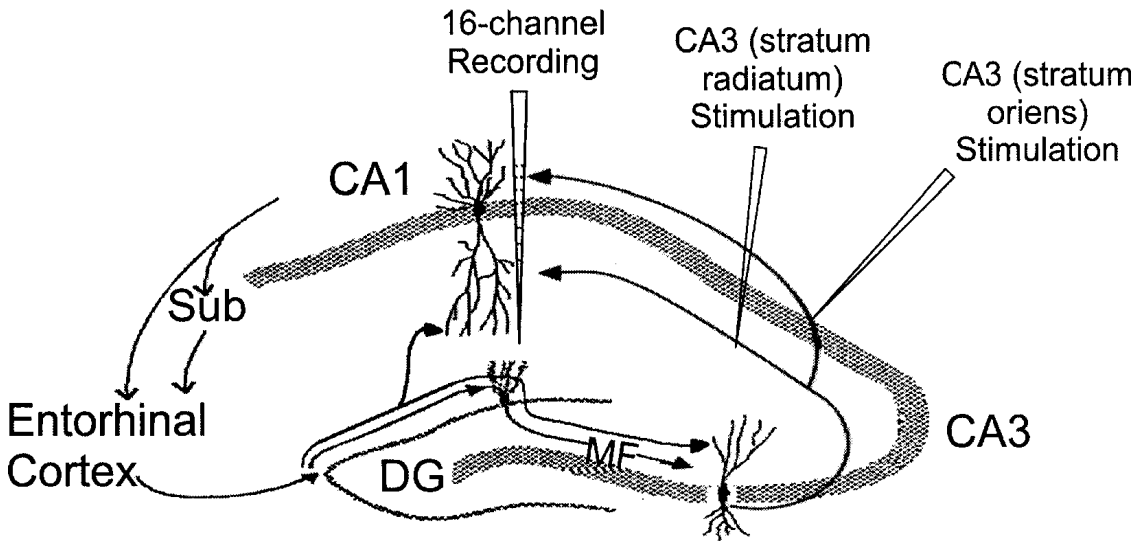

Figure 4. *A transverse section of the hippocampus illustrating the position of the stimulating electrodes (CA3 stratum radiatum or stratum oriens stimulation) and the 16-channel recording electrode.* Stimulation of the CA3 stratum oriens activated the afferents to the basal dendrites located in stratum oriens of CA1. Stimulation of the CA3 stratum radiatum activated the afferents to the apical dendrites located in the stratum radiatum of the CA1. The recording electrode spanning the stratum oriens to the stratum lacunosum-moleculare recorded evoked potentials at both basal and apical dendrites of the CA1 pyramidal cells.

2.3 Experimental Paradigm

2.3.1 Electrophysiology

Extracellular field excitatory post-synaptic potentials (fEPSPs) were recorded in CA1 pyramidal cells following activation of the CA3 stratum radiatum or stratum oriens (Kloosterman et al., 2001). Recordings were taken from a 16-channel silicon recording probe that spanned the basal and apical dendrites of the CA1 pyramidal cells. The signals were amplified 200-1000x by preamplifier and amplifier and acquired by custom made software using Tucker Davis Technologies (TDT, FL) real-time processor system RA-16. Stimulus currents were delivered (with pulse duration of 0.2 ms and intensity ranging from 45 μA to 150 μA) through a photo-isolated stimulus isolation unit (PSIU6, Astro-Med/Grass Instrument). Stimulation repetition rate was <0.1 Hz.

2.3.2 Experiments

High-intensity stimulation of CA3 stratum radiatum (typically 150-300 μA, evoking 50-75% of the maximum PS amplitude) evoked a PS that originated at the CA1 proximal apical dendrites and propagated into the basal dendrites. Similarly, high-intensity stimulation of CA3 stratum oriens evoked a PS that originated at the CA1 basal dendrites and propagated into the proximal apical dendrites. Low-intensity stimulation (typically 60-90 μA, which is around twice the threshold for a visually detectable population EPSP) in the stratum oriens and stratum radiatum of CA3 evoked an excitatory sink at the CA1 basal dendrites and proximal apical dendrites, respectively.

Low-intensity stimulation was used as the test pulse (around 2 times threshold). Recordings occurred every 5 minutes consisting of an average of 4 traces. A baseline recording consisted of thirty minutes of stable responses to excitation at the basal and apical dendrites, delivered at 0.1 Hz, which was based upon the level of consistency between slope and amplitude measurements.

After confirmation of a stable baseline, one of three synaptic plasticity inducing protocols was given to the CA1 basal/apical dendrites: Excitation-Spike Pairing (ES-Pairing), Primed Burst Stimulation (PBS), or Paired Pulse Depression (PPD) protocol. During ES-Pairing, a low-intensity excitation (E) was time-shifted with respect to a PS (Spike S) evoking high-intensity stimulation. For the first series of experiments, the low intensity stimulation generated excitation (pEPSP) at the CA1 basal dendrites and the high-intensity stimulation activated a PS in the CA1 apical dendrites that invaded into the basal dendrites. As a result, a peak of the spike was timed with the maximal sink of the EPSP in the basal dendrites through ES-Pairing. There were 5 groups of ES-Pairing at different timing intervals. Groups given 'negative' (-) ES-Pairing had a PS generated 20 ms or 10 ms before the synaptic excitation (-20 ES Interval and -10 ES Interval). Groups given 'positive' (+) ES-Pairing had a synaptic excitation generated 20 ms or 10 ms before the PS (+20 ES Interval and +10 ES Interval). The group that was given a coincident PS and synaptic excitation also falls under the positive ES-Pairing group (0 ES Interval). These ES-Pairing pairs were repeated 50 times at 5 Hz. In control conditions, only the stratum oriens stimuli (Low Basal Stimulation Only) or stratum radiatum stimuli (High Apical Stimulation Only) of ES-Pairing were given.

In another series of experiments, ES-Pairing was given to the apical dendrites. During ES-Pairing, one low-intensity stimulation to CA3a stratum radiatum was given coincident with high-intensity stimulation to CA3b stratum oriens. The low intensity stimulation generated a pEPSP in CA1 apical dendrites and the high-intensity stimulation activated a PS in the CA1 basal dendrites that invaded into the proximal apical dendrites. As a result, the peak of the spike was timed with the maximal sink of the pEPSP in the apical dendrites through ES-Pairing. Only coincident ES-Pairing was tested, in which a coincident PS and synaptic excitation was given (0 ms ES Interval). This ES-Pairing pair was repeated 50 times at 5 Hz. In control conditions, only the stratum oriens stimuli (High Basal Stimulation Only) or stratum radiatum stimuli (Low Apical Stimulation Only) of ES-Pairing were given.

In PBS experiments, a burst of excitatory afferents to the basal dendrites (4 pulses @ 100 Hz) stimulated was given coincident with the PS initiated by high-intensity apical dendritic excitation produced by a single pulse. These burst-PS pairs were repeated 60 times at 1 Hz or at 0.5 Hz.

In PPD experiments, the protocol used was first described by Thiels et al. (1994). 150-200 paired pulse stimulations at 0.5 Hz and high-intensity, separated by 25 ms, were given to the apical dendrites or the basal dendrites.

Immediately following the ES-Pairing, PBS, or PPD protocol, a 2 h response recording was conducted consisting of the same low-intensity test pulse during the baseline given every 5 minutes at low-frequency (0.1 Hz).

2.4 Confirmation of Electrode Location

2.4.1 Perfusion

After an experiment, the sites of the stimulating electrodes were lesioned by passing 0.5 mA current for 0.5 s duration. The rat was then intracardially perfused with 50 ml of saline followed by 50 ml of 4% formaldehyde solution. The brain was removed from the cranium and placed in a 4% formaldehyde solution for a minimum of 24 hours prior to sectioning.

2.4.2 Histology and Staining

Brains were frozen on the cryostat and sliced into 40 μm thick coronal sections. Brain slices were mounted onto slides and later stained with thionin. The stimulus and recording electrode locations were identified and confirmed using a light microscope (**Fig. 5**).

2.5 Inclusion Criteria

The criteria for the inclusion of experiments in the analysis were consistent among all experiments and include pre-induction, during induction, and post-induction standards. Measurements of slope were taken from all levels of the basal and apical sinks. If the baseline of a specific measure was unstable, the baseline recording was run for

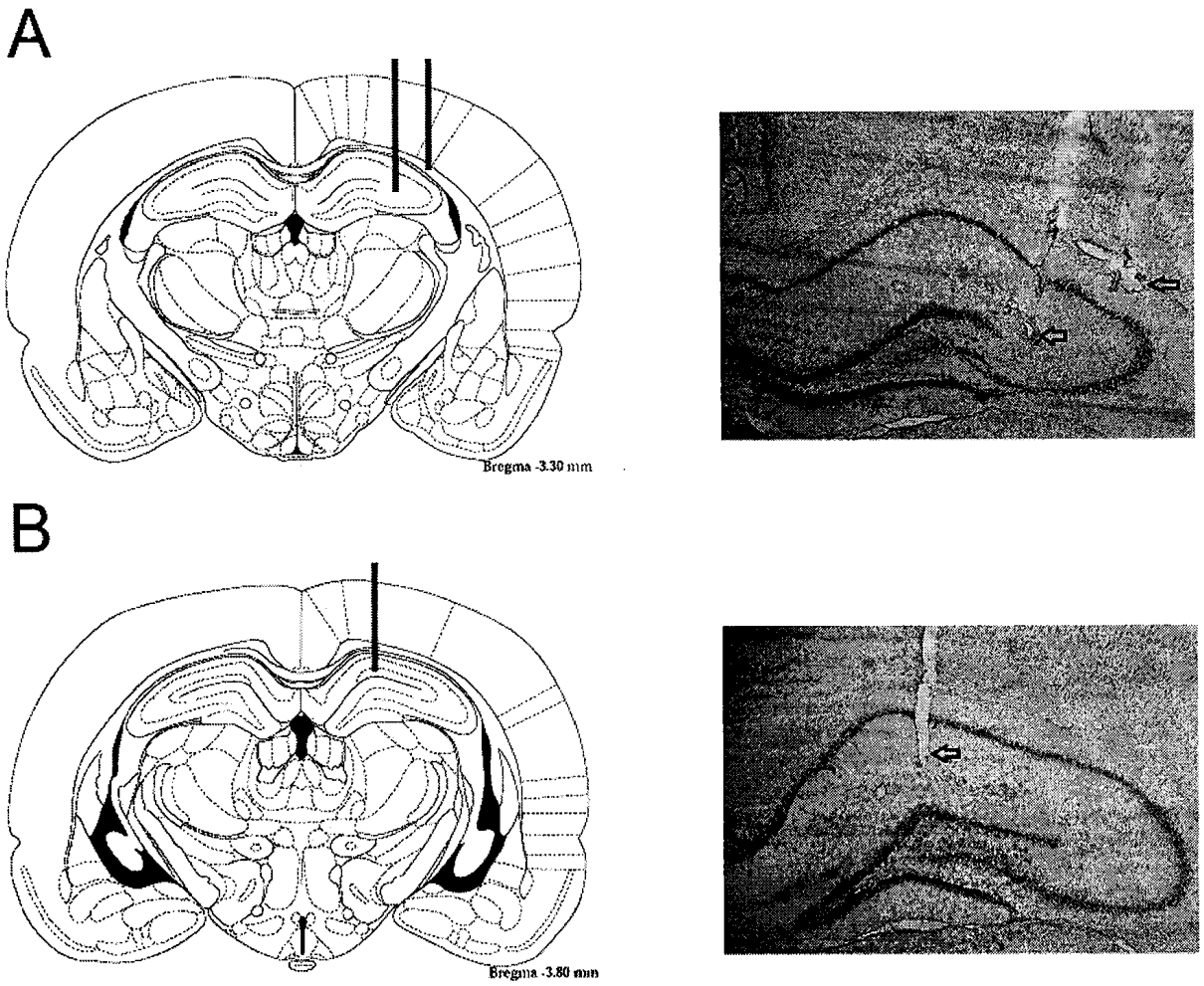

Figure 5. *Transverse hippocampal slices indicating electrode location.* Locations were based on coordinates taken from Paxinos and Watson (1986). Schematic hippocampal slices on left illustrating stimulating and recoding electrode locations (designated by solid line) and examples of corresponding thionin stained sections on right from one representative animal (TKF190). **A:** Placement of the two stimulating electrodes in CA3 with the stratum oriens coordinate at (P3.2, L3.2) and stratum radiatum coordinate at (P3.2, L2.2). Lesions made through the stimulating electrode tips are marked with arrows. The ventral coordinates varied between animals and averaged 3 mm below the skull surface for the stratum oriens stimulating electrode and 3.5 mm for the stratum radiatum stimulating electrode. **B:** Placement of the CA1 recording electrode at coordinate (P3.8, L1.8). The arrow marks the most ventral location of the track made by the recording electrode, at approximately 3.5 mm below the skull surface.

longer until 30 minutes of stable baseline was determined. The entire duration of the induction of ES-Pairing or PBS was monitored closely to make sure there were no epileptiform or spontaneous PS discharges. Also, the experiment would not be included if the stimulus intensity used during the induction did not generate a PS.

The apical and basal sinks were summed together respectively to eliminate some aspects of the shifting of the 16-channel recording electrode during the experiment. However, if after induction, the recording electrode shifted more than 1-2 channels up or down, either the basal response or apical response may shift out of recording view. These experiments where channel shifting was large were not included in the group analysis.

2.6 Analysis and Statistics

Average evoked potentials (AEPs) (N=4 sweeps) were acquired. Current Source Density (CSD), or the local measure of current source and current sink, was calculated from the evoked potentials. Since synaptic and action currents spread in the extracellular medium, a field potential does not indicate a local current, an effect which is called volume conduction. CSD removes the effects of volume conduction. A one-dimensional CSD was calculated from the field potential. CSD(z,t) as a function of depth z and time t was calculated by a second-order differencing formula (Freeman and Nicholson 1975, Leung, 2010):

$$CSD(z, t) = \sigma [2 \Phi(z, t) - \Phi(z + \Delta z, t) - \Phi(z - \Delta z, t)] / (\Delta z)^2 \qquad \text{(Equation 1)}$$

Where $\Phi(z,t)$ is the potential at depth z and time t, Δz is the spacing (50 μm) between adjacent electrodes on the 16-channel probe. The conductivity σ was assumed to be constant and the CSDs were reported in units of V/mm^2.

The slopes of the excitatory sinks in both the apical and basal dendrites were quantified from CSDs derived from AEPs (**Fig. 6**). Slope measurements were taken over a 1 ms time interval over the rising phase of the excitatory sink. The maximal slope value over 1 ms was taken as the estimate of the slope. Each measure of the excitatory sink was normalized by the grand average of the measure during baseline before LTP induction. The measure of variability was calculated as the standard error of the mean. The analysis involved every 5 minute time point of the baseline (-30 to -5 minutes) and post tetanus responses (1 minute and 5 to 120 minutes). Repeated measures analysis of variance (ANOVA) was used for statistical analysis of the normalized data at different times. If a significant main or interaction effect was found, Newman-Keuls post-hoc test was applied. $p < 0.05$ was considered statistically significant.

Comparisons were made between each ES-Pairing group and each control group (High Apical Stimulation Only and Low Basal Stimulation Only) for Basal ES-Pairing. For Apical ES-Pairing, comparisons were made between 0 ms ES-Pairing group (coincident pairing) and the control groups (High Basal Stimulation Only and Low Apical Stimulation Only). The two controls in each case were also compared to ensure that there was no difference between them. For all ES Interval and control groups, the basal and apical excitatory sink slopes after the induction protocol were compared against their own excitatory sink slopes during the baseline. Since there were no controls for PBS

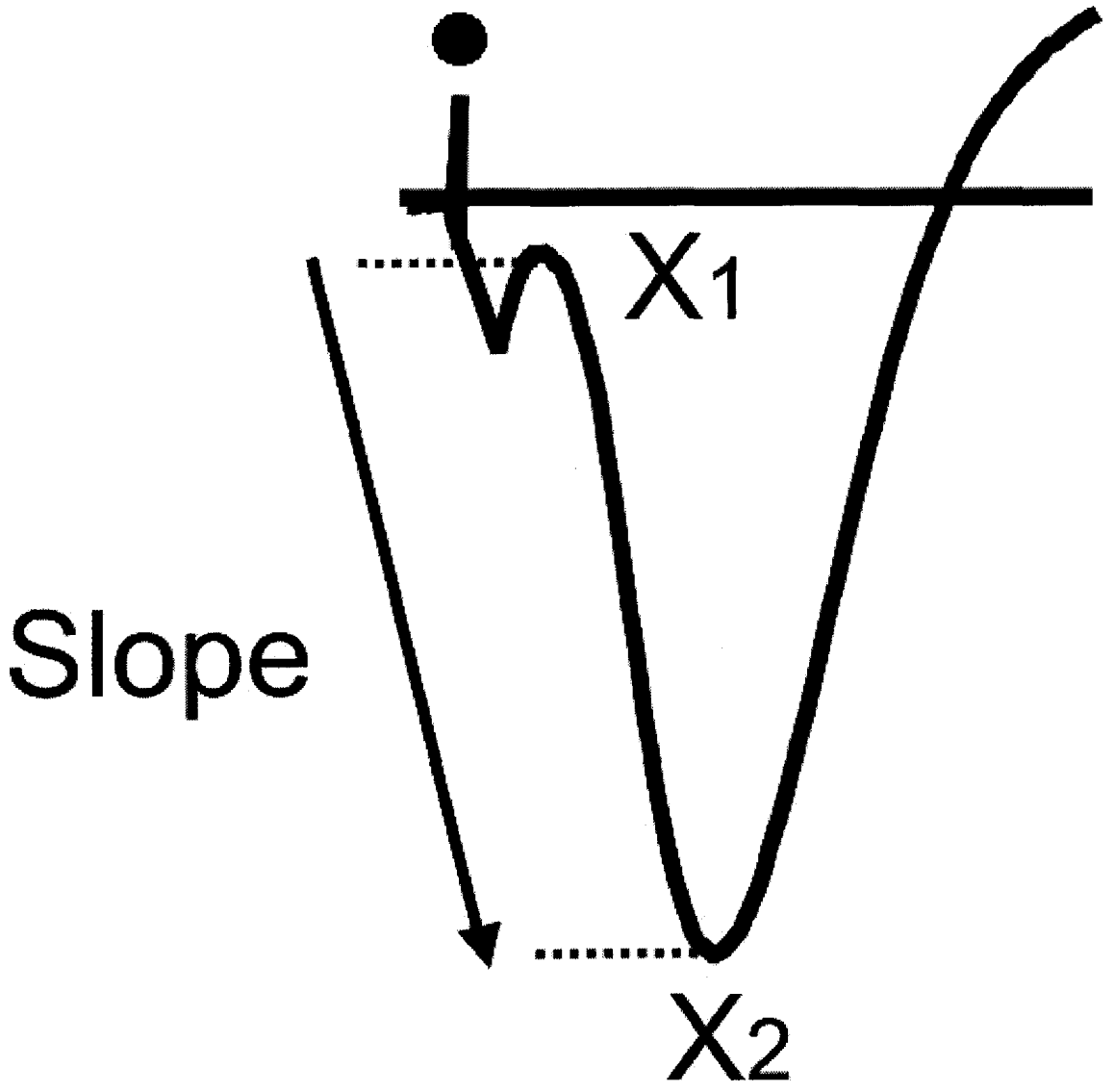

Figure 6. *Slope measurement taken from CSD derived from AEPs.* For all experiments, the slope of the excitatory sink (CSD) was calculated at 1 ms intervals for the whole duration of the rising phase of the excitatory sink (X1 to X2), and the value of the maximal magnitude of the slope was taken as the estimate of the slope. The filled circle indicates the shock artifact.

and PPD experiments, all apical and basal excitatory sink slopes after either PBS or PPD were compared against their own excitatory sink slopes during the baseline.

3. RESULTS

3.1 Basal Dendritic ES-Pairing at 5 Hz

Single pulse low-intensity stimulation of the stratum oriens in CA3 evoked characteristic evoked potentials recorded by the 16-channel electrode in CA1. The evoked potential was negative at stratum oriens and positive at stratum radiatum, consistent with basal dendritic excitation of CA1 pyramidal cells (**Fig. 7A, C**). Single pulse low-intensity stimulation of the stratum radiatum in CA3 generated a negative evoked potential in the stratum radiatum and positive at the stratum oriens in CA1, consistent with apical dendritic excitation of CA1 pyramidal cells (**Fig. 7B, D**). Single pulse high-intensity stimulation of the stratum radiatum generated a PS in CA1 pyramidal cells, which propagated from the proximal apical dendrites through the cell body and into the basal dendrites (**Fig. 8A, B**).

3.1.1 Synaptic Plasticity at the Basal Dendrites

The ES-Pairing protocol involved delivering a low-intensity pulse exciting the basal dendrites time-shifted with a high-intensity pulse evoking a PS starting at the apical dendrites. These pulse pairs were repeated 50 times at 5 Hz over 10 seconds. Following ES-Pairing, all 5 groups (-20, -10, 0, +10 and +20 ms ES Interval groups) initially showed a very large potentiation of the basal excitatory sink beginning at 5 minutes compared to High Apical Stimulation Only and Low Basal Stimulation Only control groups (**Fig. 9A, B**). The initial potentiation declined for all groups, in particular for the

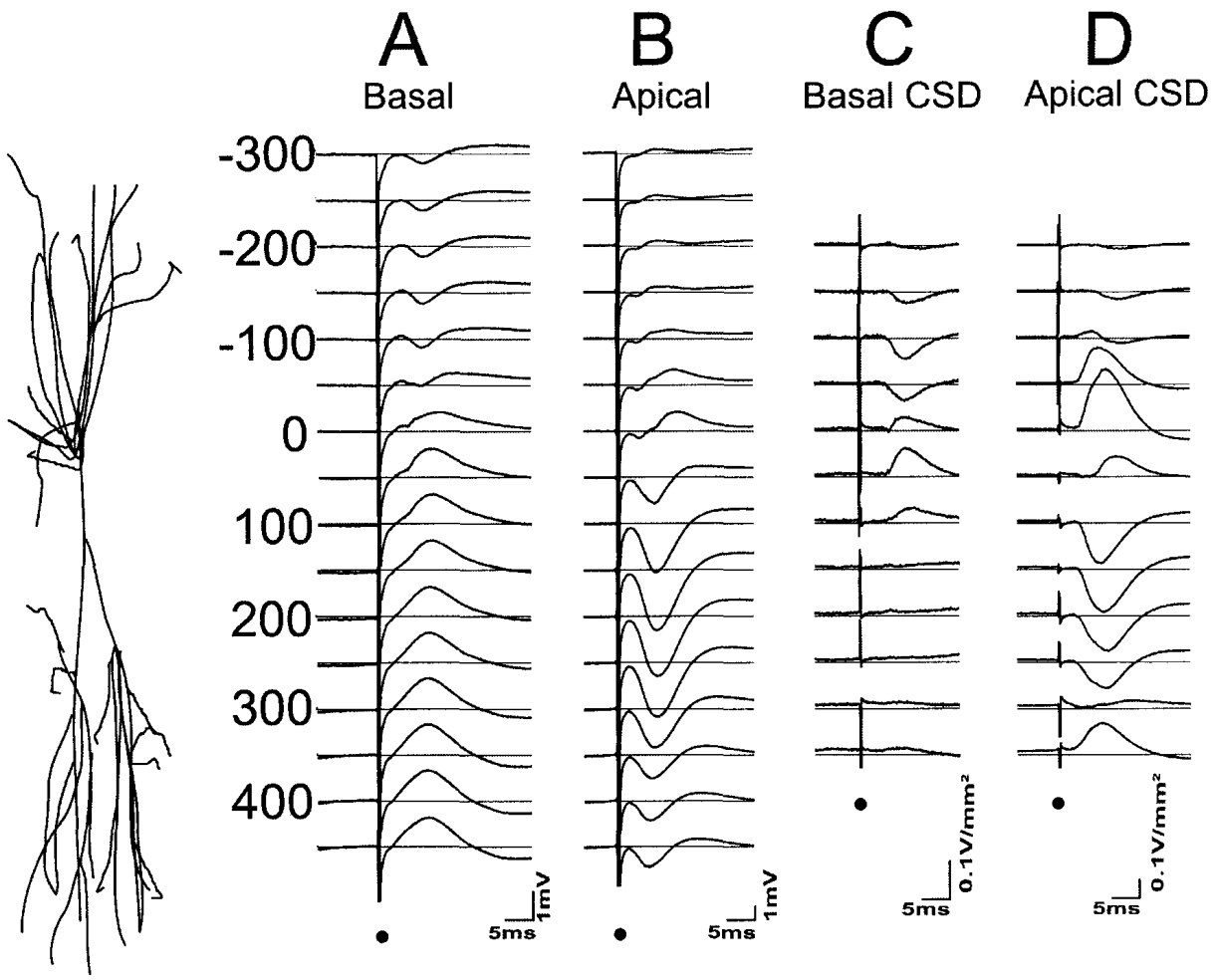

Figure 7. *Average evoked potentials (AEPs; A and B) and current source density (CSD; C and D) transients in CA1 of a representative rat (TKF208) following basal orthodromic (A and C) or apical orthodromic excitation (B and D).* Potentials were recorded simultaneously by a 16-channel electrode silicon probe with 50 μm interval between electrodes. Depths are indicated by the schematic CA1 pyramidal cell drawn and by the distance (in μm) away from the cell body layer (+ toward the apical dendrites). **A:** AEPs (average of 4 sweeps) following stimulation of the CA3 stratum oriens at 75 μA (2 times threshold). Artifacts are indicated by the solid circle underneath. **B:** Apical dendritic response as a result of CA3 stratum radiatum low intensity stimulation at 120 μA (2 times threshold). **C:** CSD profiles derived from the AEPs shown in *A*. Stimulation of the CA3 stratum oriens generated a negative sink in the CA1 basal dendrites. **D:** CSD profiles derived from the AEPs shown in *B*. Stimulation of the CA3 stratum radiatum generated a negative sink in the CA1 apical dendrites.

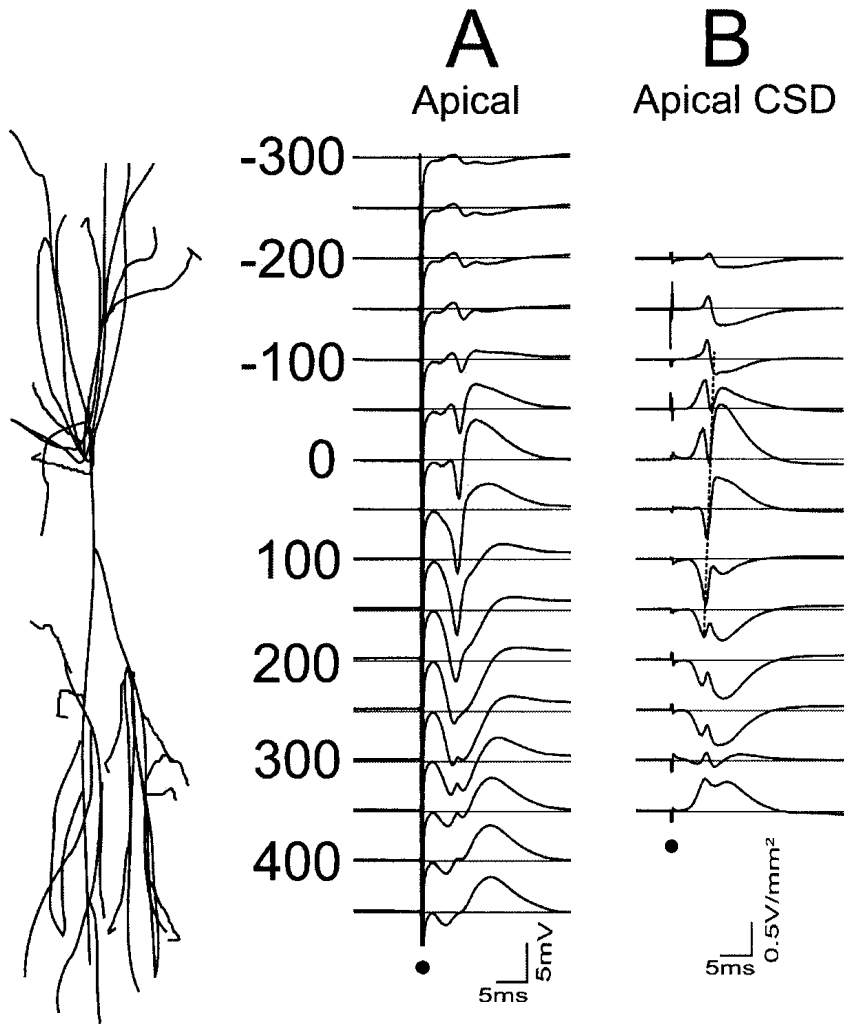

Figure 8. *Average evoked potentials (AEPs; A) and current source density (CSD; B) transients in CA1 of a representative rat (TKF208) following apical orthodromic excitation.* Potentials were recorded simultaneously by a 16-channel electrode silicon probe with 50 μm interval between electrodes. Depths are indicated by the schematic CA1 pyramidal cell drawn and by the distance (in μm) away from the cell body layer (+ toward the apical dendrites). Population spike peaks are linked with a dotted line, indicating propagation direction. **A:** AEPs (average of 4 sweeps) following stimulation of the CA3 stratum radiatum at 300 μA (evoking 50% of the maximum population spike amplitude). Artifacts are indicated by the solid circle underneath. **B:** CSD profiles derived from the AEPs shown in *A*. Stimulation of the stratum radiatum in CA3 generated an apical dendritic spike in CA1 at 150 μm that propagated into the cell bodies and then into the basal dendrites.

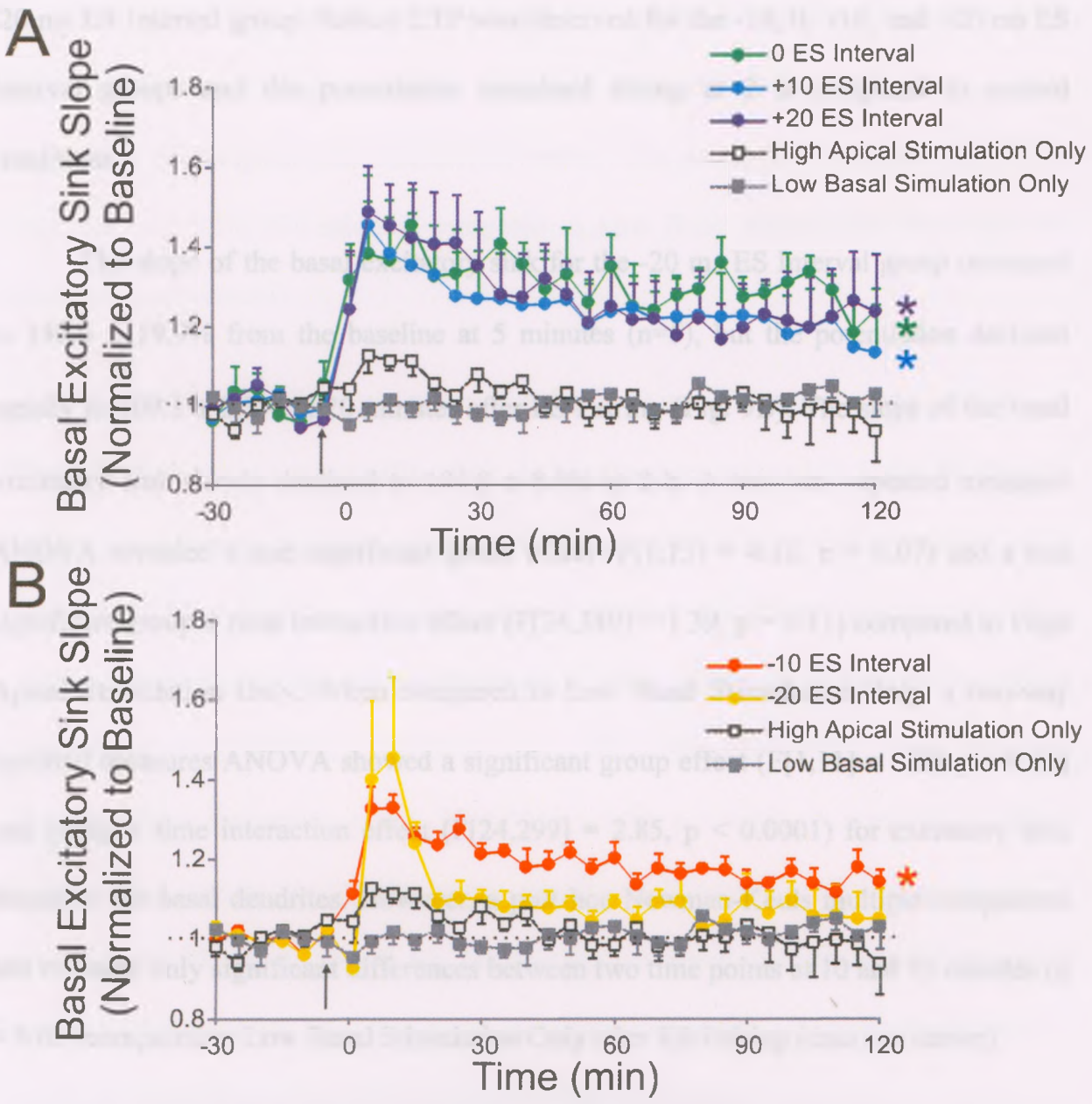

Figure 9. *CA1 basal dendritic LTP following basal ES-Pairing.* Each point represents the normalized value relative to the average measure of the baseline before time = 0 (ES-Pairing indicated with an arrow). **A:** Positive ES-Pairing in the basal dendrites resulted in a significant potentiation of the basal excitatory sink for 0, +10, and +20 ES Interval groups for 2 h (LTP magnitude at 2 h was 123.5 ± 5.9%, n=6; 113.4 ± 12.0%, n=7; 123.7 ± 14.6%, n=5; respectively) compared to control groups: 102.9 ± 5.3%, n=7 (Low Basal Stimulation Only); 93.6 ± 7.5%, n=9 (High Apical Stimulation Only). **B:** Negative ES-Pairing in the basal dendrites resulted in a significant potentiation of the basal excitatory sink only for -10 ES Interval group for 2 h (LTP magnitude at 2 h was 114.3 ± 3.3%) compared to control groups. ES-Pairing at -20 ES Interval did not result in significant potentiation compared to controls (104.8 ± 7.9%, n=5). * represents significant difference between an ES Interval group vs. High Apical Simulation Only condition.

-20 ms ES Interval group. Robust LTP was observed for the -10, 0, +10, and +20 ms ES Interval groups and the potentiation remained strong at 2 h compared to control conditions.

The slope of the basal excitatory sink for the -20 ms ES Interval group increased to 140.0 ± 19.9% from the baseline at 5 minutes (n=5), but the potentiation declined rapidly to 109.1 ± 2.3% at 20 minutes after ES-Pairing (**Fig. 9B**). The slope of the basal excitatory sink slowly declined to 104.8 ± 8.9% at 2 h. A two-way repeated measures ANOVA revealed a non significant group effect ($F[1,13] = 4.12$, $p = 0.07$) and a non significant group x time interaction effect ($F[24,349] = 1.39$, $p = 0.11$) compared to High Apical Stimulation Only. When compared to Low Basal Stimulation Only, a two-way repeated measures ANOVA showed a significant group effect ($F[1,11] = 8.29$, $p < 0.05$) and group x time interaction effect ($F[24,299] = 2.85$, $p < 0.0001$) for excitatory sink slopes in the basal dendrites. However, a post-hoc Newman-Keuls multiple comparison test revealed only significant differences between two time points at 10 and 15 minutes ($p < 0.05$) compared to Low Basal Stimulation Only after ES-Pairing (data not shown).

The slope of the basal excitatory sink for the -10 ms ES Interval group increased to a maximum of 132.8 ± 5.6% (n=5) at 5 minutes (**Fig. 9B**). At 2 h, the slope was at 114.3 ± 3.3% from the baseline. A two-way repeated measures ANOVA revealed a significant group effect ($F[1,13] = 21.07$, $p < 0.001$), but no group x time interaction effect ($F[24,349] = 0.65$, $p = 0.89$) compared to High Apical Stimulation Only. It also showed a significant group effect ($F[1,11] = 37.74$, $p < 0.001$) and group x time interaction effect ($F[24,299] = 3.57$, $p < 0.0001$) when compared to Low Basal

Stimulation Only. A post-hoc Newman-Keuls multiple comparison test showed a significant difference at time points 5, 10, 25, 60, 70, 100, 115 and 120 min ($p < 0.05$) compared to High Apical Stimulation Only and all time points (1-120 minutes; $p < 0.05$) except for 105, 110, 120 minutes compared to Low Basal Stimulation Only after ES Pairing (data not shown).

The slope of the basal excitatory sink for the 0 ms ES Interval group increased to 131.6 ± 9.1% (n=6) at 1 minute (**Fig. 9A**). At 2 h, the slope was at 123.5 ± 5.9% from the baseline. A two-way repeated measures ANOVA revealed a significant group effect ($F[1,14] = 41.57$, $p < 0.0001$), but no group x time interaction effect ($F[24,374] = 0.40$, $p = 1.00$) compared to High Apical Stimulation Only. When compared to Low Basal Stimulation Only, it showed a significant group effect ($F[1,12] = 48.03$, $p < 0.0001$), but no group x time interaction effect ($F[24,324] = 1.09$, $p = 0.35$). A post-hoc Newman-Keuls multiple comparison test disclosed a significant difference at all time points (1-120 minutes, $p < 0.05$) except for 65, 90, 115 minutes compared to High Apical Stimulation Only and all time points (1-120 minutes; $p < 0.05$) except for 115 minutes compared to Low Basal Stimulation Only after ES-Pairing (data not shown).

The slope of the basal excitatory sink for the +10 ms ES Interval group increased to a maximum of 145.3 ± 13.0% (n=7) of the baseline at 5 minutes and remained elevated at 113.4 ± 12.0% of the baseline at 2 h (**Fig. 9A**). A two-way repeated measures ANOVA revealed a significant group effect ($F[1,15] = 5.44$, $p < 0.05$), but no group x time interaction effect ($F[24,399] = 0.46$, $p = 0.99$) compared to High Apical Stimulation Only. When compared to Low Basal Stimulation Only, there was a significant group

effect ($F[1,13] = 5.01$, $p < 0.05$) and group x time interaction effect ($F[24,349] = 4.06$, $p < 0.0001$). A post-hoc Newman-Keuls multiple comparison test disclosed a significant difference at all time points (1-120 minutes; $p < 0.05$) except for 115 minutes compared to High Apical Stimulation Only and all time points (1-120 minutes; $p < 0.05$) except for 115 and 120 minutes compared to Low Basal Stimulation Only after ES-Pairing (data not shown).

The slope of the basal excitatory sink increased to a maximum of 148.8 ± 11.9% (n=5) at 5 minutes after ES-Pairing at +20 ms Interval (**Fig. 9A**). At 2 h, the slope was at 123.7 ± 14.6% from the baseline. A representative experiment is shown in **Figure 10A, B**. A two-way repeated measures ANOVA revealed a significant group effect ($F[1,13] = 8.87$, $p < 0.05$), but no group x time effect ($F[24,349] = 1.13$, $p = 0.31$) compared to High Apical Stimulation Only. When compared to Low Basal Stimulation Only, there was a significant group effect ($F[1,11] = 8.35$, $p < 0.05$) and group x time interaction effect ($F[24,299] = 4.88$, $p < 0.0001$). A post-hoc Newman-Keuls multiple comparisons test disclosed a significant difference at all time points (1-120 minutes; $p < 0.05$) except for 1, 40, 65, 75, 85, 90, 105 minutes compared to High Apical Stimulation Only and at all time points after ES-Pairing (1-120 minutes; $p < 0.05$) compared to Low Basal Stimulation Only (data not shown).

For the control condition of High Apical Stimulation Only, the basal excitatory sink slope increased to a maximum of 112.7 ± 4.4% (n=9) at 5 minutes and dropped to 0.94 ± 7.5% at 2 h (**Fig. 9A, B**). In contrast, Low Basal Stimulation Only had a slope of

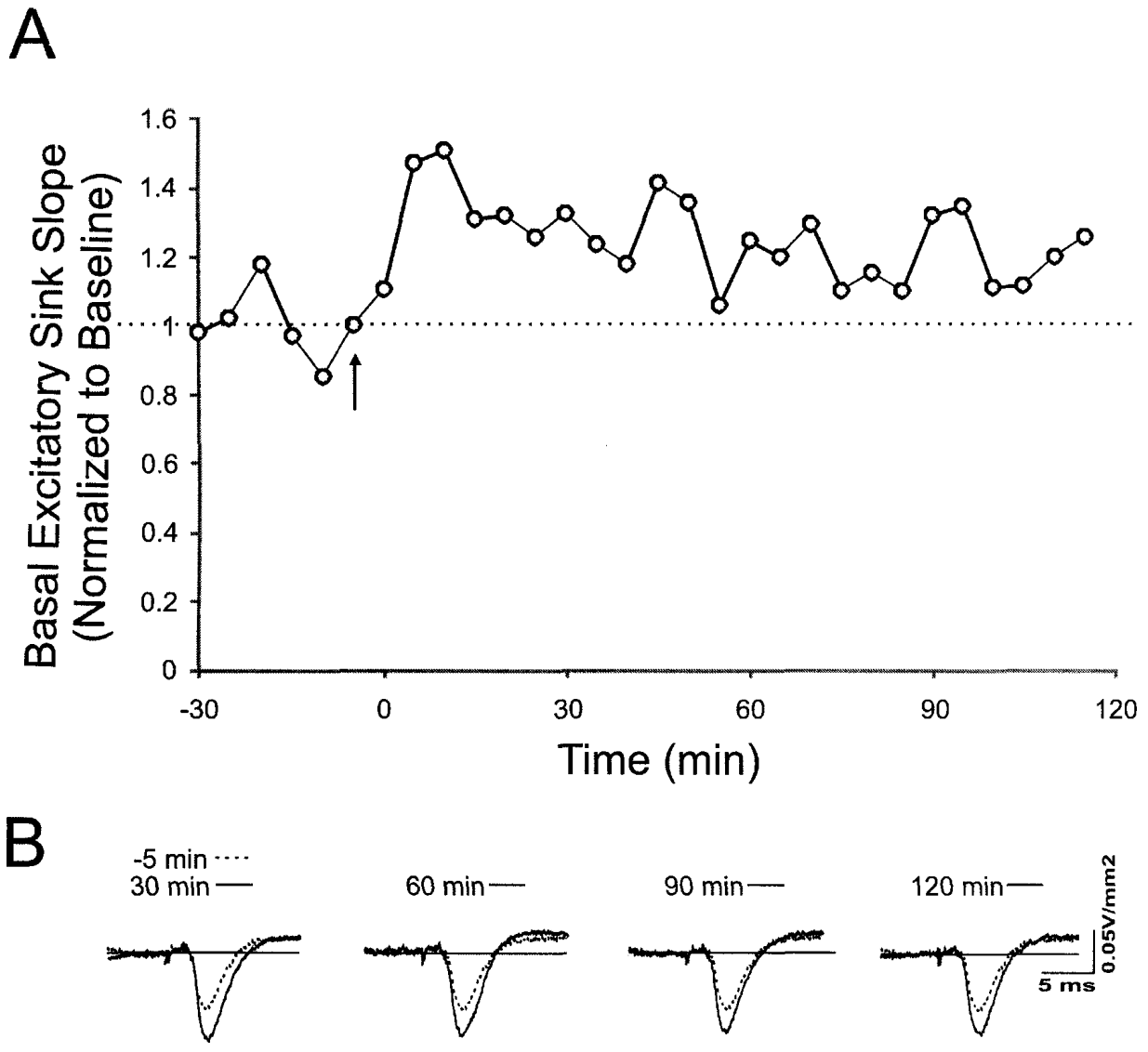

Figure 10. *+20 ms ES-Pairing for a representative rat (TKF208).* **A:** A graphical representation of a single experiment showing the potentiation of the basal excitatory sink slope for 2 h after ES-Pairing at +20ms (indicated with an arrow). An average evoked potential (n=4 sweeps) was recorded every five minutes and the basal dendritic sink was analyzed and normalized by the average baseline basal dendritic sink before time = 0. **B:** the average basal excitatory sinks are illustrated for the last point in the baseline (-5 min; dotted line) and at 30, 60, 90 and 120 min (solid line) following +20 ES-Pairing. The potentiation at all 4 time points is robust.

101.7 ± 2.7% (n=7) at 5 minutes and 102.9 ± 5.3% at 2 h (**Fig. 9A, B**). A two-way repeated measures ANOVA revealed no significant group effect ($F[1,12] = 0.28$, $p = 0.61$), but did reveal a group x time interaction effect ($F[24,399] = 1.74$, $p < 0.05$). However, post-hoc Newman-Keuls multiple comparison test revealed no significant differences at any time point. All groups that showed significant differences compared to controls (-10, 0, +10, and +20 ES Interval) also showed significant differences compared to their own baseline (data not shown).

3.1.2 Synaptic Plasticity at the Apical Dendrites

The slope of the apical dendritic sinks after the ES-Pairing in the basal dendrites showed a slight potentiation beginning at 5 min following ES-Pairing in all 5 groups (-20, -10, 0, +10 and +20 ms ES Interval), compared to Low Basal Stimulation Only, but not High Apical Stimulation Only. Similarly, the apical dendritic sink after High Apical Stimulation Only control showed potentiation at beginning at 5 minutes also (**Fig. 11A, B**). Although, the initial potentiation for all groups declined with time, potentiation was found for -20, -10, +10, and +20 ES Interval groups up to 110 min only against Low Basal Stimulation Only.

The slope of the apical excitatory sink for the -20 ms ES Interval group increased to a maximum of 121.9 ± 6.9% (n=5) of the baseline at 10 minutes (**Fig. 11B**). The potentiation declined quickly to 109.3 ± 4.4% at 20 minutes and at 2 h the slope was at 102.5 ± 4.7%. A two-way repeated measures ANOVA did not reveal a significant group

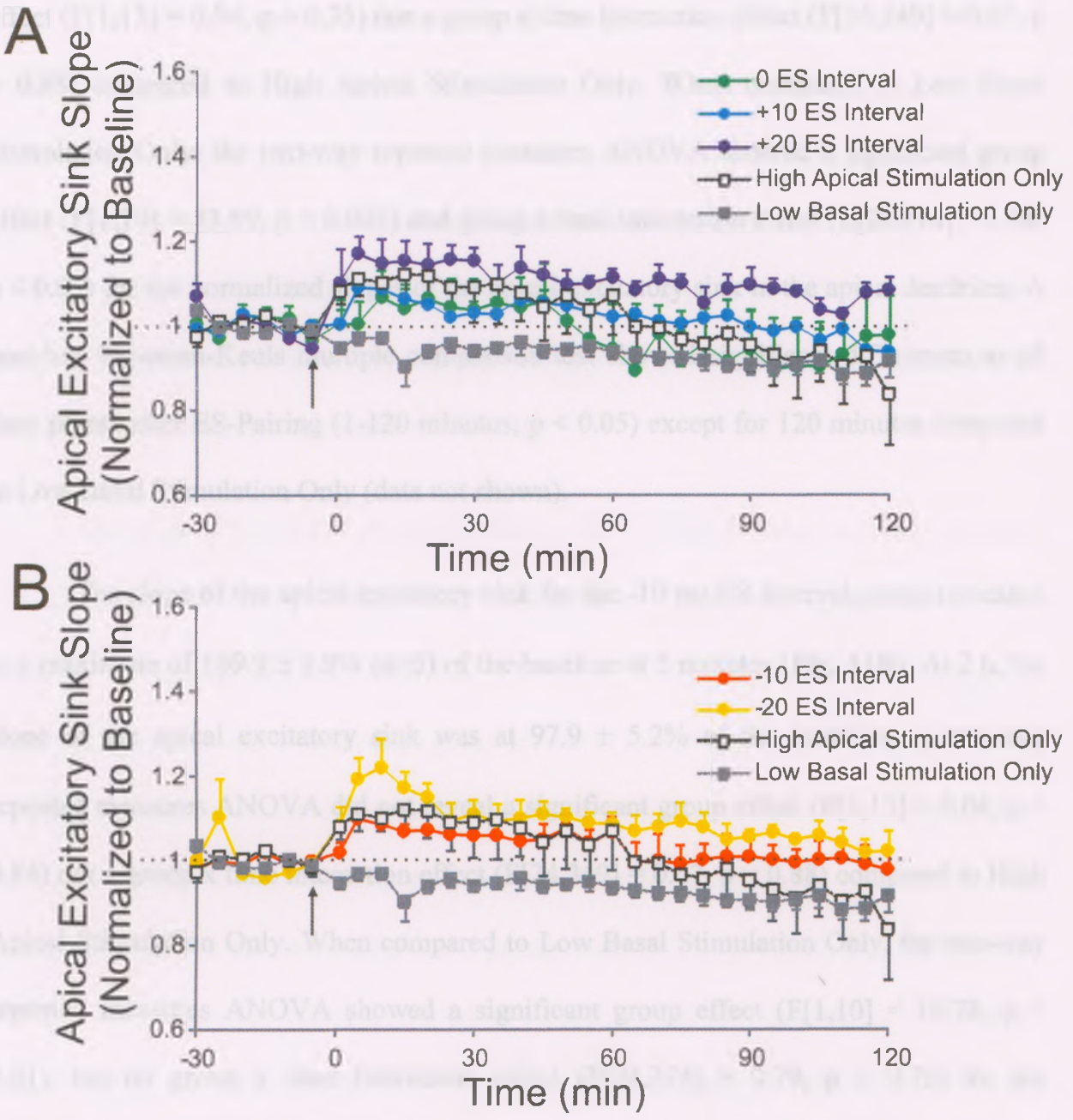

Figure 11. *Apical dendritic excitatory sink measured in CA1 following basal ES-Pairing.* Each point represents the normalized value relative to the average measure of the baseline before time = 0 (ES-Pairing indicated with an arrow). **A:** Positive ES-Pairing in the basal dendrites resulted in no significant potentiation of the apical excitatory sink for 0, +10, and +20 ES Interval groups for 2 h compared to High Apical Stimulation Only. **B:** Negative ES-Pairing in the basal dendrites resulted in no significant potentiation of the apical excitatory sink for -10 and -20 ES Interval group for 2 h compared to High Apical Stimulation Only. Statistical significant differences were found between all ES Interval groups vs. Low Basal Simulation Only condition and vs. baseline.

effect ($F[1,13] = 0.94$, $p = 0.35$) nor a group x time interaction effect ($F[24,349] = 0.67$, $p = 0.88$) compared to High Apical Stimulation Only. When compared to Low Basal Stimulation Only, the two-way repeated measures ANOVA showed a significant group effect ($F[1,10] = 33.99$, $p < 0.001$) and group x time interaction effect ($F[24,274] = 1.58$, $p < 0.05$) for the normalized slopes of the apical excitatory sink in the apical dendrites. A post-hoc Newman-Keuls multiple comparison test showed significant differences at all time points after ES-Pairing (1-120 minutes; $p < 0.05$) except for 120 minutes compared to Low Basal Stimulation Only (data not shown).

The slope of the apical excitatory sink for the -10 ms ES Interval group increased to a maximum of 109.9 ± 1.9% (n=5) of the baseline at 5 minutes (**Fig. 11B**). At 2 h, the slope of the apical excitatory sink was at 97.9 ± 5.2% of the baseline. A two-way repeated measures ANOVA did not reveal a significant group effect ($F[1,13] = 0.04$, $p = 0.84$) nor a group x time interaction effect ($F[24,349] = 0.67$, $p = 0.88$) compared to High Apical Stimulation Only. When compared to Low Basal Stimulation Only, the two-way repeated measures ANOVA showed a significant group effect ($F[1,10] = 10.78$, $p < 0.01$), but no group x time interaction effect ($F[24,274] = 0.79$, $p = 0.75$) for the normalized excitatory sink slopes in the apical dendrites. A post-hoc Newman-Keuls multiple comparison test revealed significant differences at time points 5-35, 45, 50, 60, 90, 110 and 115 minutes ($p < 0.05$) compared to Low Basal Stimulation Only after ES-Pairing (data not shown).

The slope of the apical excitatory sink for the 0 ms ES Interval group increased to a maximum of 106.9 ± 6.3% (n=6) of the baseline at 5 minutes (**Fig. 11A**). At 2 h, the

slope of the Apical excitatory sink was at 97.7 ± 9.3%. A two-way repeated measures ANOVA did not reveal a significant group effect ($F[1,14] = 0.16$, $p = 0.69$) nor a group x time interaction effect ($F[24,374] = 0.73$, $p = 0.82$) compared to High Apical Stimulation Only. When compared to Low Basal Stimulation Only, the two-way repeated measures ANOVA also did not reveal a significant group effect ($F[1,11] = 0.58$, $p = 0.47$) nor a group x time interaction effect ($F[24,299] = 1.22$, $p = 0.23$) for the normalized excitatory sink slopes in the apical dendrites.

The slope of the apical excitatory sink for the +10 ms ES Interval group increased to a maximum of 109.1 ± 3.1% (n=7) of the baseline at 5 minutes (**Fig. 11A**). At 2 h, the slope of the apical excitatory sink was 93.7 ± 4.5%. A two-way repeated measures ANOVA did not reveal a significant group effect ($F[1,15] = 0.002$, $p = 0.97$) nor a group x time interaction effect ($F[24,399] = 1.01$, $p = 0.45$) compared to High Apical Stimulation Only. When compared to Low Basal Stimulation Only, the two-way repeated measures ANOVA showed a significant group effect ($F[1,12] = 8.60$, $p < 0.05$), but no group x time interaction effect ($F[24,324] = 1.16$, $p = 0.28$) for the normalized excitatory sink slopes in the apical dendrites. A post-hoc Newman-Keuls multiple comparison test showed significant differences at time points 5-20, 45-55, 80, 85 and 110 minutes ($p < 0.05$) compared to Low Basal Stimulation Only after ES-Pairing (data not shown).

The slope of the apical excitatory sink for the +20 ms ES Interval group increased to a maximum of 116.9 ± 4.3% (n=5) from the baseline at 5 minutes (**Fig. 11A**). The potentiation declined slowly and at 2 h, the slope of the apical excitatory sink was 108.3 ± 3.1%. A two-way repeated measures ANOVA did not reveal a significant group effect

($F[1,12] = 1.27$, $p = 0.28$) nor a group x time interaction effect ($F[24,324] = 0.53$, $p = 0.97$) compared to High Apical Stimulation Only. When compared to Low Basal Stimulation Only, the two-way repeated measures ANOVA showed a significant group effect ($F[1,12] = 33.7$, $p < 0.001$), but no group x time interaction effect ($F[24,349] = 1.32$, $p = 0.16$) for the normalized excitatory sink slopes in the apical dendrites. A post-hoc Newman-Keuls multiple comparison test showed significant differences at all time points (1-120 minutes; $p < 0.05$) compared to Low Basal Stimulation Only after ES-Pairing (data not shown).

There were small changes in the excitatory sinks in the control experiments. The apical excitatory sink slope during High Apical Stimulation Only increased to 111.2 ± 4.0% (n=9) at 1 minute and at 2 h, it was at 83.7 ± 11.8% (**Fig. 11A, B**). In contrast, Low Basal Stimulation Only had a slope of 94.6 ± 1.1% (n=6) at 1 minute and at 2 h, the slope was at 91.8 ± 3.8% (**Fig. 11A, B**). A two-way repeated measures ANOVA did not reveal significant differences between the two control conditions (High Apical Stimulation Only and Low Basal Stimulation Only), in either the main (group) effect ($F[1,14] = 1.56$, $p = 0.23$) nor a group x time interaction effect ($F[24,374] = 1.31$, $p = 0.15$). Also, all groups not including the control groups (-20, -10, 0, +10, and +20 ES Interval), showed significant differences compared to their own baseline (data not shown).

3.1.3 Summary

ES-Pairing in the basal dendrites resulted in LTP at 2 h with a potentiation of the basal excitatory sink slope of ~1.2 times the baseline for 4 of the 5 groups (-10, 0, +10 and +20 ms ES Interval) compared to both control groups and compared to baseline. The -20 ES Interval group showed only STP of about 20 minutes when compared to the Low Basal Stimulation Only and no LTP at 2 h when compared to both controls. The same ES-Pairing that induced LTP in the basal dendrites did not potentiate the apical excitatory sink slope in any of the 5 groups at 2 h compared to High Apical Stimulation Only. However, when compared to Low Basal Stimulation Only, 4 of the 5 groups (-20, -10, +10 and +20 ms ES Interval) were potentiated and all 5 groups were potentiated compared to their own baseline. A comparison of the two controls revealed only a significant time effect and no group effect or group x interaction effect. Although the effect of ES-Pairing in the 5 groups follows High Apical Stimulation Only control closely and the initial potentiation decreased back to baseline at 2 h for all groups, the potentiation shown when comparing each group to its own baseline cannot be ignored. Taken together, these results demonstrate that ES-Pairing within 20 ms given to the basal dendrites induces LTP in the basal dendrites, but LTP is favoured more by positive ES-Pairing (**Fig. 12A-D**). ES-Pairing in the basal dendrites also results in potentiation of the apical dendrites regardless of the timing.

3.2 Basal Dendritic Primed Burst Stimulation

Primed Burst Stimulation (PBS) consisted of a burst of excitatory afferents to the basal dendrites (4 pulses @ 100 Hz) stimulated coincident with a backpropagated PS

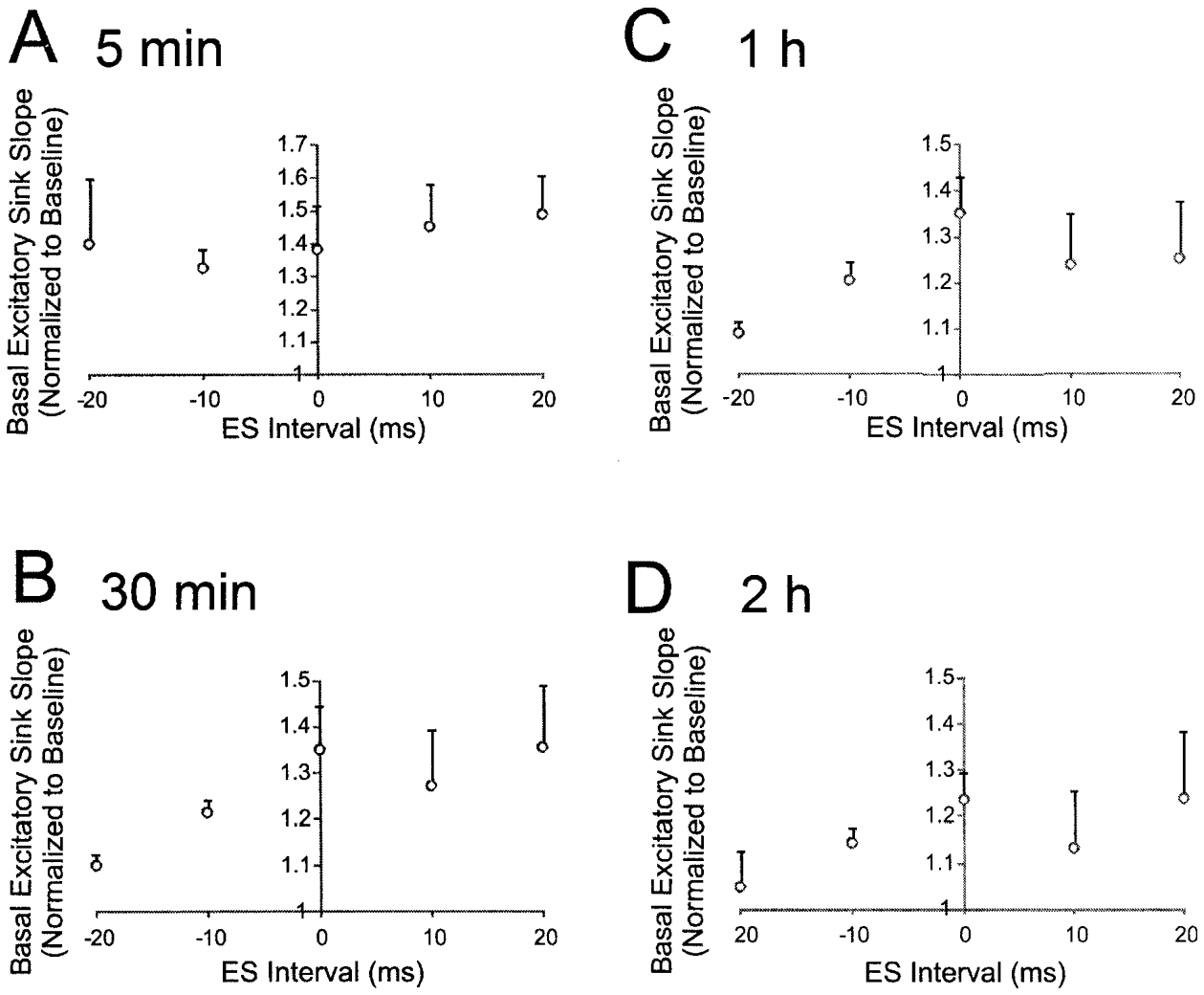

Figure 12. *Magnitude of potentiation of the basal dendritic sink (mean plus standard error of the mean) induced by pairing at* different *ES Intervals at* ***A:*** *5 min,* ***B:*** *30 min,* ***C:*** *1 h, and* ***D:*** *2 h following basal ES-Pairing.* -20 ES-Pairing resulted in potentiation of the basal excitatory sink at 5 min but rapidly declined to near baseline by 30 min. In contrast, -10, 0, +10, and +20 ms ES-Pairing resulted in potentiation of the excitatory sink slope at 5 min, which remained potentiated for 2 h.

initiated by a single-pulse high-intensity stimulation to the apical dendrites. These burst-PS pairs were repeated 60 times at 1 Hz or 0.5 Hz.

3.2.1 PBS at 1 Hz

Immediately following PBS, there was a large potentiation of the basal excitatory sink which was maintained for 2 h compared to the apical excitatory sink (**Fig. 13**). At 1 minute following PBS, the slope of the basal excitatory sink increased to 168.5 ± 28.3% (n=4) from the baseline. At 2 h, the basal excitatory sink magnitude was at 165.9 ± 12.0%. In comparison, the apical excitatory sink slope at 1 minute after PBS was at 91.5 ± 4.3% (n=4) and at 2 h the measurement was 91.9 ± 15.1%. A one-way repeated measures ANOVA revealed a significant group effect ($F[1,29] = 3.19$, $p < 0.05$) for the basal excitatory sink slope after PBS compared to baseline. However, there was no significant difference for the apical excitatory sink slope after PBS compared to baseline ($F[1,29] = 0.50$, $p = 0.98$). A post-hoc Newman-Keuls multiple comparison test showed significant differences for basal excitatory sink slopes at time points 1, 15, 25 and 70 minutes ($p < 0.05$) compared to the baseline (**Fig. 13**). During PBS, some spontaneous PS discharges occurred for at least 160 ms after the start of each primed burst (**Fig. 14**).

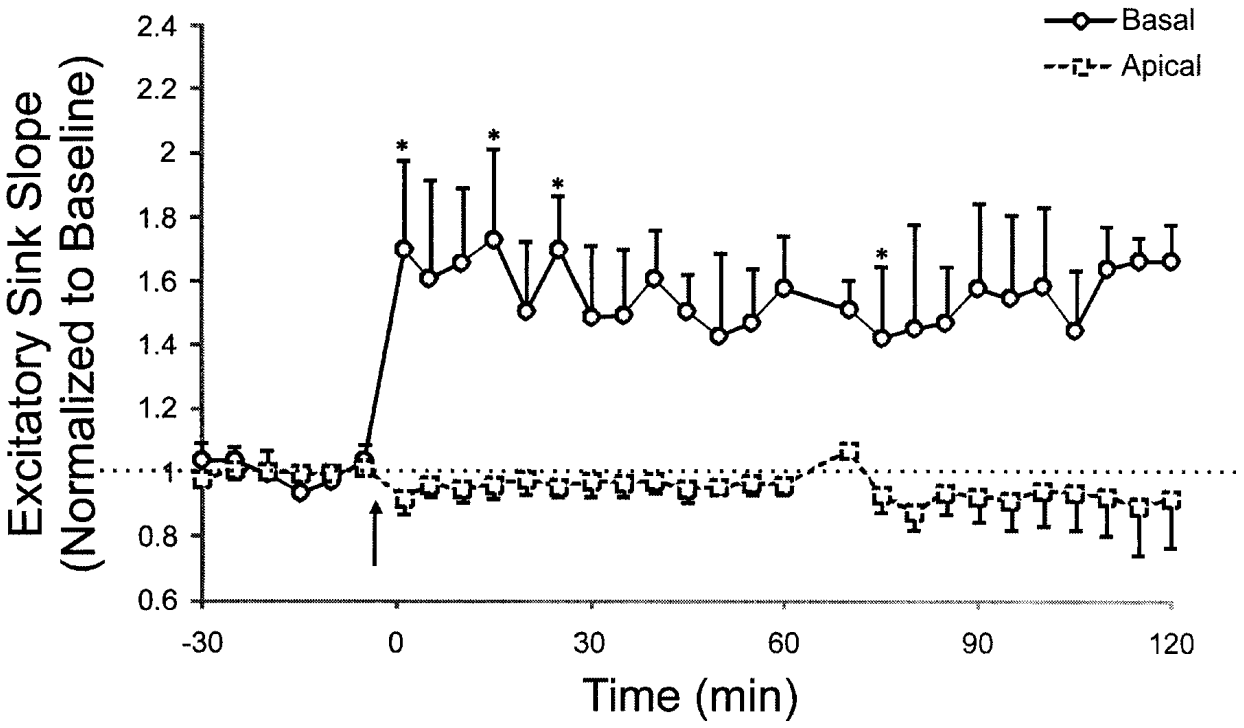

Figure 13. *Pairing an apical backpropagated spike in the basal dendrites with a burst of basal dendritic excitatory sinks at 1 Hz resulted in LTP of the basal dendrites, but not the apical dendrites.* High intensity stimulation of the CA3 stratum radiatum evoked a population spike that initiated in the CA1 apical dendrites and propagated into the basal dendrites. A low-intensity burst stimulation (4 pulses at 100 Hz) of CA3 stratum oriens, which generated subthreshold excitatory sinks in the CA1 basal dendrites, was paired simultaneously (zero time delay) with a backpropagated PS initiated by the high-intensity apical dendritic excitation; pairing was given at 1 Hz for 60 seconds (60 times). The slope of the basal dendritic sink in CSD increased significantly (165.9 ± 12.0%; n=4) compared to baseline for 2 h. In contrast, the slope of the apical dendritic sink was at 91.9 ± 15.1% (n=4) after the PBS at 2 h (* represents post-hoc significances following repeated measures ANOVA).

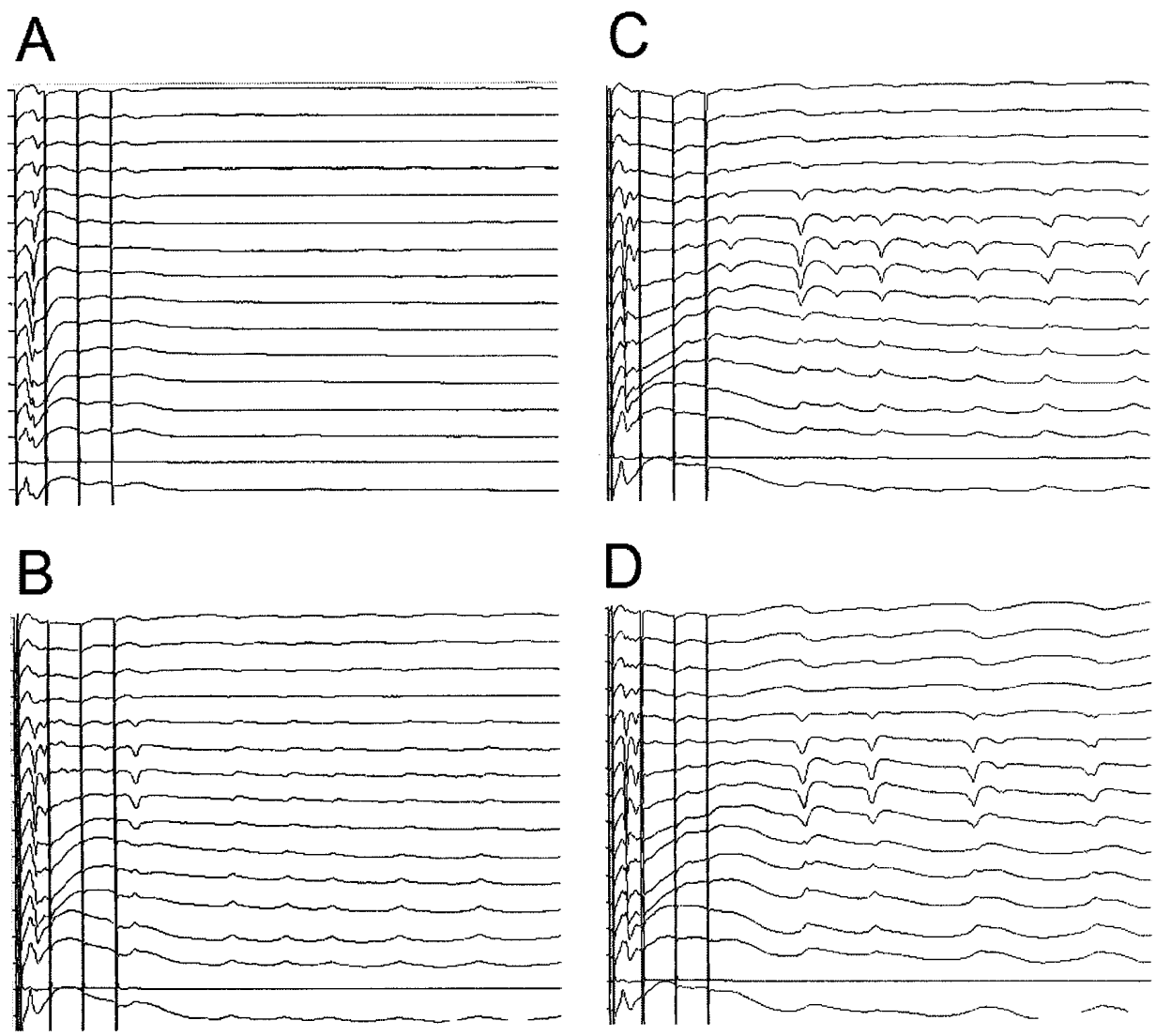

Figure 14. *Traces taken during the induction of 1 Hz primed burst stimulation (PBS) for a representative rat (TKF060).* PBS included a low-intensity 4-pulse burst given to the CA3 stratum oriens at 100 Hz given coincident with a backpropagated population spike (PS) initiated by a high-intensity apical dendritic excitation. The burst and the apical stimulation were given at 1 Hz for 60 seconds (60 times). The traces were recorded at **A:** the 5th trace, **B:** the 15th trace, **C:** the 20th trace and **D:** the 25th trace. Each trace has a duration of 160 ms. Spontaneous PS discharges during the PBS induction occurred starting at the 5th trace (*B*) and was still present at the 25th trace (*D*).

3.2.2 PBS at 0.5 Hz

Lowering the frequency of the PBS to 0.5 Hz resulted in no spontaneous PS discharges during induction, but also resulted in no potentiation of the basal excitatory sink for 2 h compared to the apical excitatory sink (**Fig. 15**). At 1 minute following PBS, the slope of the basal excitatory sink was 86.6 ± 6.4% (n=6) from the baseline. At 2 h, the basal excitatory sink magnitude was at 97.9 ± 14.2%. In comparison, the apical excitatory sink slope at 1 minute after PBS was at 91.8 ± 0.9% (n=5) and at 2 h the measurement was 106.5 ± 4.6%. A one-way repeated measures ANOVA revealed no significant group effect for basal ($F[1,30] = 0.97$, $p = 0.51$), but did reveal a significant group effect for apical ($F[1,30] = 2.31$, $p < 0.05$) excitatory sink slope after PBS compared to baseline. However a post-hoc Newman-Keuls multiple comparison test showed no significant differences at any time points compared to baseline (**Fig. 15**).

3.2.3 Summary

Coincident pairing of backpropagated PS in the basal dendrites with a burst of stimulation of the excitatory afferents to the basal dendrites at 1 Hz induced LTP specifically at the basal dendrites. However, because of the spontaneous spiking during PBS induction, the LTP could be attributed to the 1Hz-PBS protocol, which may allow frequency facilitation of the response and thus a small after-discharge. Thus, the after-discharge may induce LTP of the basal dendrites as opposed to the pairing protocol itself. Since the pattern of the spontaneous spiking was variable, it was difficult to design a

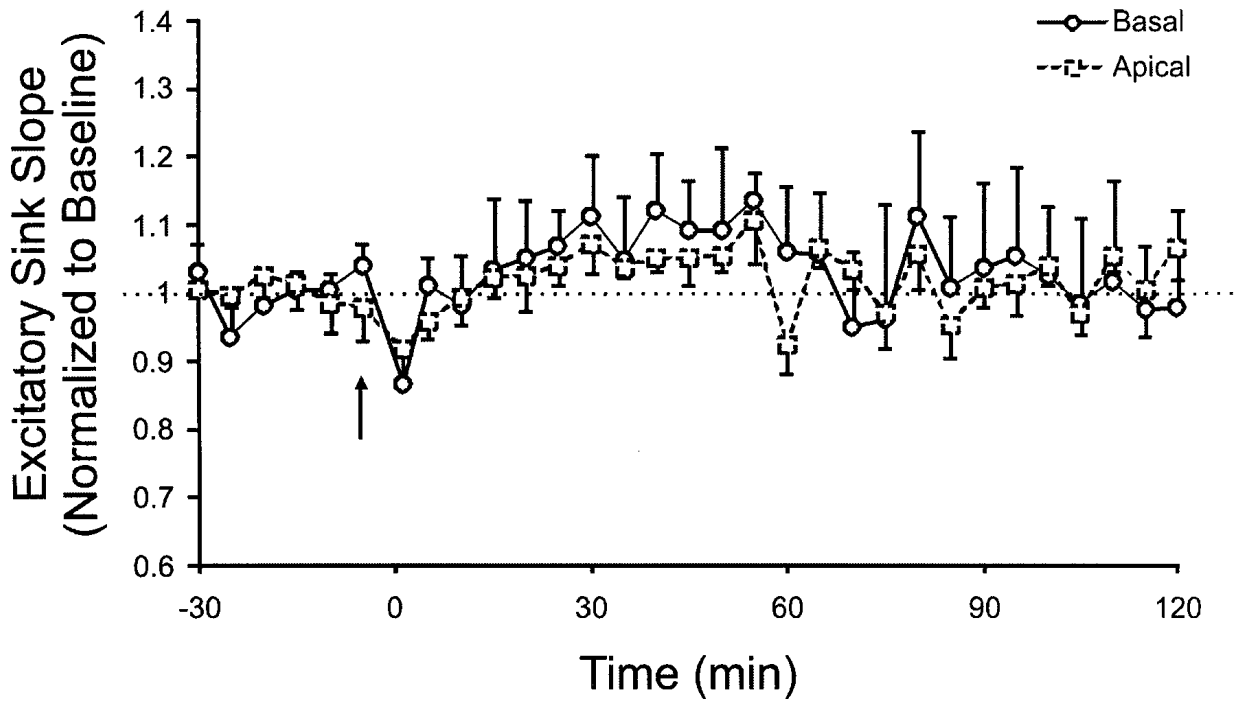

Figure 15. *Pairing an apical backpropagated spike in the basal dendrites with a burst of basal dendritic excitatory sinks at 0.5 Hz did not result in LTP of the basal dendrites nor the apical dendrites.* High intensity stimulation of the CA3 stratum radiatum evoked a PS that initiated in the CA1 apical dendrites and propagated into the basal dendrites. A low-intensity burst stimulation (4 pulses at 100 Hz) of CA3 stratum oriens, which generated subthreshold excitatory sinks in the CA1 basal dendrites, was paired simultaneously (zero time delay) with a backpropagated PS initiated by the high-intensity apical dendritic excitation; pairing was given at 0.5 Hz for 60 seconds (60 times). The slope of the basal dendritic sink in CSD (97.9 ± 14.2%) showed no significant increase compared to baseline. The apical dendritic sink was 106.5 ± 4.6% compared to baseline 2 h after the primed burst stimulation.

control experiment without pairing but with spontaneous spiking. When the PBS frequency was lowered, coincident pairing of a backpropagated apical spike in the basal dendrites with a burst of EPSPs in the basal dendrites at 0.5 Hz did not induce LTP at the basal dendrites.

3.3 Apical Dendritic ES-Pairing at 5 Hz

Single pulse low-intensity stimulation of the stratum oriens and stratum radiatum in CA3 evoked characteristic evoked potentials recorded by the 16 channel electrode in CA1 as mentioned in *4.1 (Basal Dendritic ES-Pairing 5 Hz)* (**Fig. 7A, B, C, D**). Single pulse high-intensity stimulation of the stratum oriens generated a PS in the basal dendrites of CA1 pyramidal cells, which propagated through the cell body and into the apical dendrites (**Fig. 16A, B**). LTP was categorized as a robust increase in the slope of the apical excitatory sink of CA1 pyramidal neurons generated by single pulse low-intensity stimulations in CA3. LTP was determined if the increase in slope persisted for 2 h.

3.3.1 Synaptic Plasticity at the Apical Dendrites

ES-Pairing in the apical dendrites included one low intensity pulse given to the apical dendrites simultaneous with a high-intensity pulse given to the basal dendrites. These pairs were repeated 50 times at 5 Hz over 10 seconds. 0 ms ES-Pairing of the

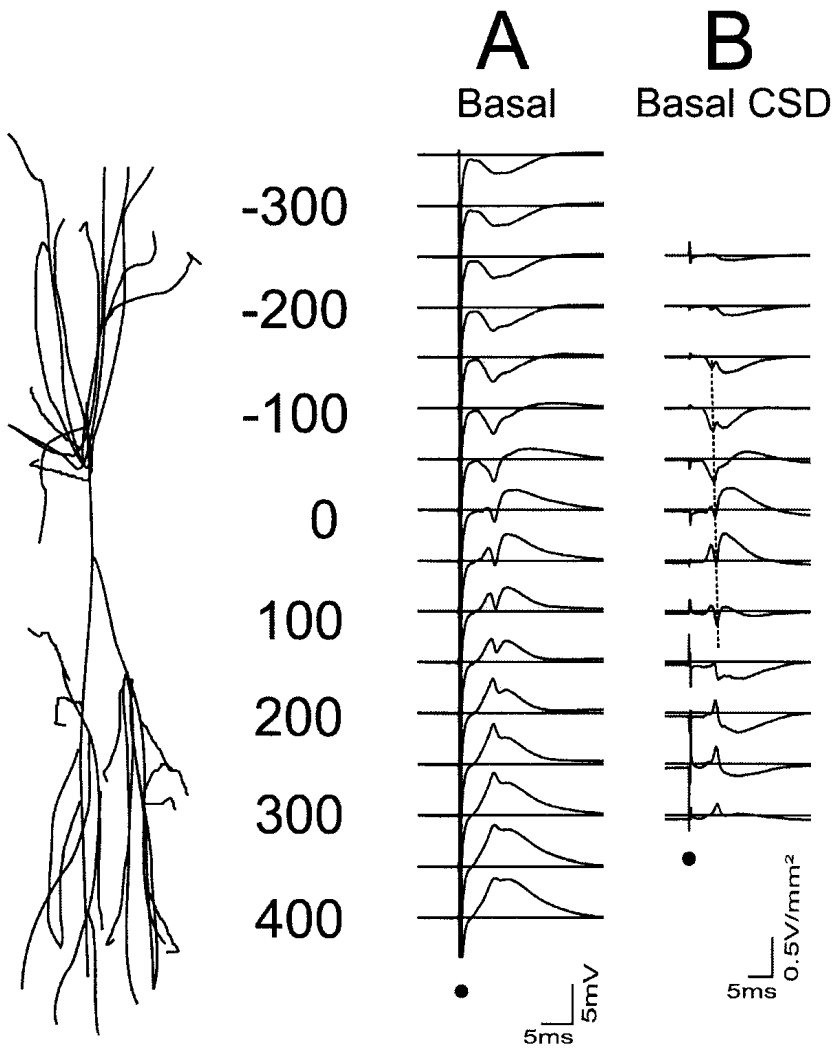

Figure 16. *Average evoked potentials (AEPs; A) and current source density (CSD; B) transients in CA1 of 1 rat (TKF174) following apical orthodromic excitation.* Potentials were recorded simultaneously by a 16-channel electrode silicon probe with 50 μm interval between electrodes. Depths are indicated by the schematic CA1 pyramidal cell drawn and by the distance (in μm) away from the cell body layer (+ toward the apical dendrites). Spike peaks are linked with a dotted line, indicating propagation direction. **A:** AEPs (average of 4 sweeps) following stimulation of the CA3 stratum oriens at 300 μA (intensity that evoked 50% of the maximum PS). Artifacts are indicated by the solid circle underneath. **B:** CSD profiles derived from the AEPs shown in *A*. Stimulation of the stratum oriens in CA3 generated a basal dendritic spike in CA1 at 150 μm above the cell layer that propagated into the cell bodies and then into the apical dendrites.

apical dendrites resulted in LTP of the apical excitatory sink for 2 h compared to baseline (data not shown) and to Low Apical Stimulation Only and High Basal Stimulation Only control groups (**Fig. 17A**). Immediately following ES-Pairing at 1 minute, 0 ES Interval group showed a robust potentiation of the apical excitatory sink which increased to a maximum of 131.0 ± 9.9% at 10 minutes (n=7). At 2 h, the apical excitatory sink slope was at 118.1 ± 4.8%. Apical excitatory sink slope in the High Basal Stimulation Only was at 110.0 ± 20.6% (n=5) at 1 minute and 90.7 ± 11.5% at 2 h. Apical excitatory sink slope in the Low Apical Stimulation Only was at 94.1 ± 2.6% (n=3) at 1 minute and 90.1 ± 1.0% at 2 h. For 0 ES-Pairing, a two-way repeated measures ANOVA revealed a significant group effect ($F[1,11] = 6.55$, $p < 0.05$), but no group x time interaction effect ($F[24,299] = 0.84$, $p = 0.68$) compared to High Basal Stimulation Only. When compared to Low Apical Stimulation Only, the two-way repeated measures ANOVA showed a significant group effect ($F[1,9] = 9.49$, $p < 0.05$), but no group x time interaction effect ($F[24,249] = 0.35$, $p = 1.00$). A post-hoc Newman-Keuls multiple comparisons test revealed significant differences at time point 5-25, 40, 45, 55-80, 90-110, 120 minutes ($p < 0.05$) compared to High Basal Stimulation Only and significant differences at all time points (1-120; $p < 0.05$) compared to Low Apical Stimulation Only after 0 ES-Pairing (**Fig. 17A**). Apical excitatory sink slopes for 0 ES Interval also showed similar differences compared to baseline after ES-Pairing (data not shown). In addition, there are no significant differences between the two controls: group effect ($F[1,7] = 0.07$, $p = 0.80$) and group x time interaction effect ($F[24,249] = 0.33$, $p = 1.00$) (**Fig. 17A, B**).

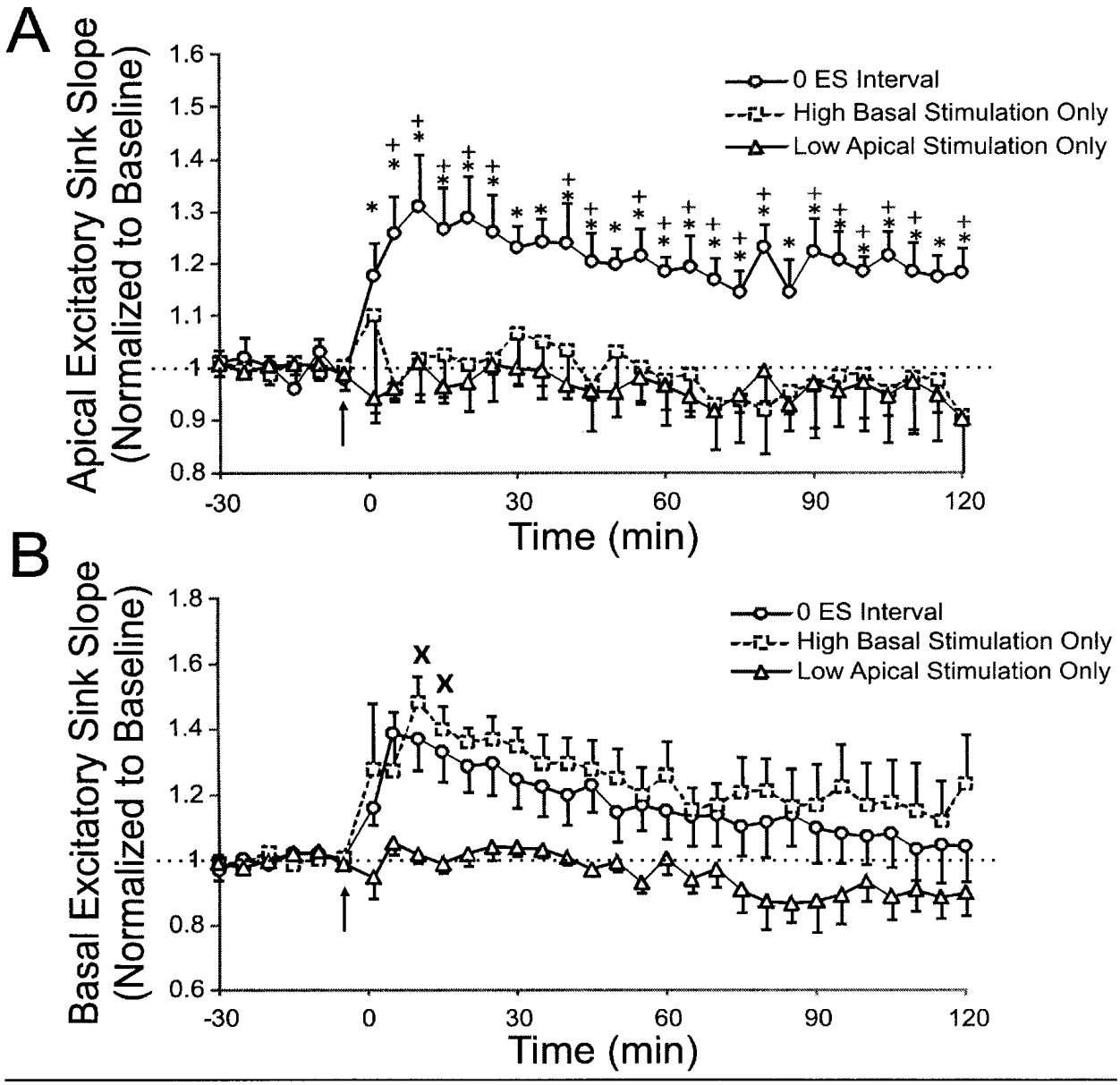

Figure 17. *0 ES-Pairing at the apical dendrites resulted in LTP of the apical dendrites and a short term potentiation of the basal dendrites.* **A:** 0 ES-Pairing (arrow above) potentiated the slope of the apical excitatory sink for 2 h (LTP magnitude at 2 h was 118.1% ± 4.8%, n=7 rats) compared to control experiments (High Basal Stimulation Only: 90.7% ± 11.5%, n=5; Low Apical Stimulation Only: 90.1% ± 10.4%, n=5). **B.** 0 ES-Pairing at the apical dendrites or High Basal Stimulation Only (arrow above), resulted in a short term potentiation of the slope of the basal excitatory sink compared to baseline but neither was significant compared to the low apical stimulation only condition. * and + represents significant difference between 0 ES Interval vs. Low Apical Stimulation Only and 0 ES Interval vs. High Basal Stimulation Only conditions, respectively ($p < 0.05$, Newman-Keuls posthoc test). **X** represents significant differences between High Basal Stimulation Only and Low Apical Stimulation Only conditions

3.3.2 Synaptic Plasticity at the Basal Dendrites

We also measured the basal excitatory sink slope during ES Pairing in the apical dendrites. Following 0 ms ES-Pairing, both the 0 ES Interval condition and the High Basal Stimulation Only condition resulted in potentiation of basal excitatory sink slope compared to baseline (data not shown) and Low Apical Stimulation Only (**Fig. 17B**). Immediately following ES-Pairing at 1 minute, 0 ES Interval group showed a robust potentiation of the basal excitatory sink which increased to a maximum of 138.4 ± 11.1% at 5 minutes (n=7). The potentiation declined slowly and at 2 h, the basal excitatory sink slope was at 104.2 ± 10.6%. The basal excitatory sink slope in the High Basal Stimulation Only followed a similar trend. The slope was at 148.0 ± 7.9% (n=5) at 10 minutes and decreased to 123.5 ± 15.0% at 2 h. In comparison, the basal excitatory sink slope in the Low Apical Stimulation Only condition was at 94.7 ± 6.6% (n=4) at 1 minute and 89.8 ± 6.7% at 2 h. For 0 ES-Pairing, a two-way repeated measures ANOVA revealed no significant group effect ($F[1,11] = 0.43$, $p = 0.53$) nor a group x time interaction effect ($F[24,299] = 0.48$, $p = 0.98$) compared to High Basal Stimulation Only. When compared to Low Apical Stimulation Only, the two-way repeated measures ANOVA also showed no significant group effect ($F[1,10] = 3.18$, $p = 0.11$) nor a group x time interaction effect ($F[24,274] = 1.55$, $p = 0.055$). Comparing the two controls, we saw a significant difference after a two-way repeated measures ANOVA in the group effect ($F[1,8] = 11.57$, $p < 0.05$), but no significant difference in the group x time interaction effect ($F[24,224] = 0.34$, $p = 1.00$). A post-hoc Newman-Keuls multiple comparisons test revealed significant differences between the two controls (High Basal Stimulation Only and Low Apical Stimulation Only) at time points 10 and 15 minutes

after 0 ES-Pairing (**Fig. 17B**). Basal excitatory sink slopes for 0 ES Interval and High Basal Stimulation Only also showed significant differences compared to baseline after ES-Pairing (data not shown).

3.3.3 Summary

The results indicated that 0 ms ES-Pairing of the apical dendrites results in LTP of the apical dendrites with a potentiation of the apical excitatory sink slope of ~1.2 times the baseline compared to both control groups. However, the same ES-Pairing that induced LTP in the apical dendrites also potentiated the basal excitatory sink slope for a short time. Although the potentiation declined over 2 h, the basal excitatory sink slope showed a large potentiation immediately after 0 ES-Pairing or High Basal Stimulation Only conditions. It seems that High Basal Stimulation Only was enough to induce LTP at the basal dendrites, but apical dendritic LTP required coincident ES-Pairing of a PS with an excitatory sink.

3.4 Paired Pulse Depression (PPD) Protocol

Paired Pulse Depression (PPD) protocol consisted of 200 pairs of high-intensity stimulation spaced 25 ms apart given at 0.5 Hz to either the apical or basal dendrites of CA1. The first stimulus generated a PS, followed by inhibition of the PS evoked by the second stimulus given 25 ms later. LTD was categorized as a robust decrease in the slope

of the apical or basal excitatory sink of CA1 pyramidal neurons generated by single pulse low-intensity stimulations in CA3. LTD was determined if the decrease in slope persisted for 2 h.

3.4.1 PPD in the Apical Dendrites

Immediately following PPD protocol, there was a large decrease of the apical excitatory sink which was maintained for 2 h compared to baseline (**Fig. 18**). At 1 minute following PPD, the slope of the apical excitatory sink decreased to 70.4 ± 3.1% (n=7) from the baseline. The slope decreased further to 62.4 ± 4.0% at 2 h. In comparison, the basal excitatory sink slope at 1 minute after PPD was at 95.8 ± 1.5% (n=6) and at 2 h the measurement was 93.0 ± 11.1%. A one-way repeated measures ANOVA revealed a significant group effect ($F[1,29] = 32.21$, $p < 0.0001$) between the slope of the apical excitatory sink before and after PPD. However, there was a non significant group effect ($F[1,29] = 0.78$, $p = 0.76$) between the slope of the basal excitatory sink before and after PPD. A post-hoc Newman-Keuls multiple comparison test showed significant differences for apical excitatory sink slopes at all time points (1-120 min, $p < 0.05$) compared to baseline (**Fig. 18**).

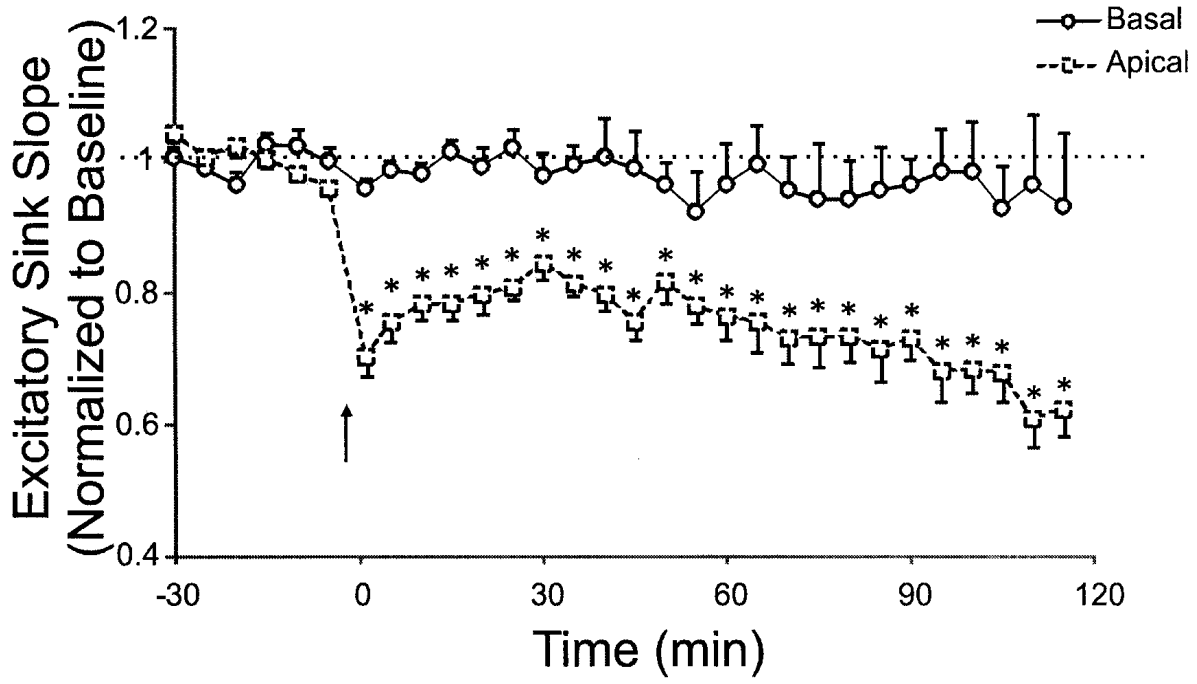

Figure 18. *Paired Pulse Depression (PPD) protocol at the apical dendrites resulted in LTD of the apical dendritic excitatory sink and no change in the basal dendritic excitatory sink.* 200 pulse pairs, 25 ms apart, delivered at time zero (arrow above) to the apical CA1 dendrites depressed the slope of the apical excitatory sink for 2 h (LTD magnitude at 2 h was 62.4% ± 4.0%, n=7 rats) compared to baseline. The basal excitatory sink remained unchanged (magnitude of the basal excitatory sink was 93.0% ± 11.1%, n=6 rats) compared to baseline. * $P<0.05$ difference, Newman-Keuls posthoc comparison between normalized apical and basal excitatory sink slopes.

3.4.2 PPD in the Basal Dendrites

After PPD protocol in the basal dendrites, there was a no change in the basal or apical excitatory sink for 2 h compared to baseline (**Fig. 19**). At 1 minute and 2 h following PPD, the slope of the basal excitatory sink was at 90.8 ± 2.1% (n=6) and increased slightly to 108.9 ± 13.4% from the baseline, respectively. Similarly, the apical excitatory sink slope at 1 minute after PPD was at 90.9 ± 4.9% (n=6) and at 2 h the measurement was 93.1 ± 19.3%. A one-way repeated measures ANOVA revealed a significant group effect ($F[1,30] = 1.79$, $p < 0.05$) between the slope of the basal excitatory sink before and after PPD and a significant group effect ($F[1,30] = 1.74$, $p < 0.05$) between the slope of the apical excitatory sink before and after PPD. However, a post-hoc Newman-Keuls multiple comparison test showed no significant differences for apical and basal excitatory sink slopes at all time points (1-120 min) compared to baseline (**Fig. 19**).

3.4.3 Summary

200 pairs of high-intensity stimulation given 25 ms apart at 0.5 Hz induced LTD specifically at the apical dendrites when given to the apical dendrites, which reproduced the results by Thiels et al. (1994). However, when the same protocol was given to the basal dendrites, there was no change to the basal excitatory sinks. In fact, there was even a small non-significant potentiation observed at 2 h. This suggests that the basal dendrites

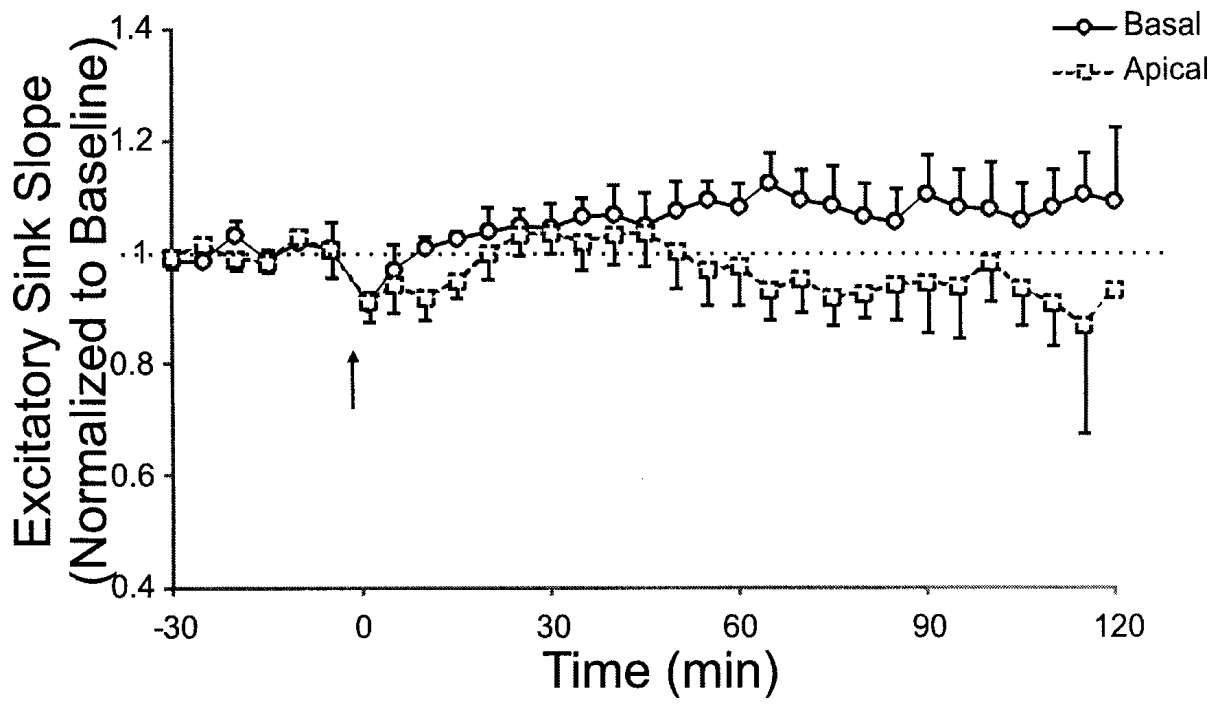

Figure 19. *Paired Pulse Depression (PPD) protocol at the basal dendrites resulted in no change of the basal or apical dendrites.* 200 pulse pairs, 25 ms apart (arrow above), given to the basal CA1 dendrites resulted in no change of the basal and apical excitatory sink (excitatory sink magnitude at 2 h was at 108.9% ± 13.4%, n=6 rats and 93.1 ± 19.3%, n=6 rats for basal and apical dendrites, respectively) compared to baseline. There were no significant differences between apical or basal excitatory sink slopes after PPD compared to baseline.

may have different receptor/channel properties than the apical dendrites that prevent LTD from being induced.

4. DISCUSSION

The timing of pre- and postsynaptic inputs is known to influence synaptic plasticity and to determine its direction. The spike-timing model, which has been extensively studied *in vitro*, has been suggested as the way synapses in the brain either get stronger or weaker, and as such, documenting that hippocampal synapses are able to potentiate or depress responses based on the timing of inputs in an *in vivo* model is essential to furthering the understanding of the mechanisms behind LTP and LTD.

The current results confirmed my first hypothesis that coincident or positive ES-Pairing induces long-term potentiation at the basal dendrites in CA1. With the second hypothesis, the results corresponded with the prediction that LTP would be induced at the CA1 basal dendrites when ES-pairing was given within 20 ms of each other. However, our results did not support our second part of the ES Interval hypothesis, which proposed that negative ES-Pairing induces long-term depression at the basal dendrites in CA1 within a 20 ms time window. Thus, there may be differences in this experimental protocol or the properties of the basal dendrites that would result in the absence of LTD observed.

Traditionally, the STDP protocol *in vitro* is performed on cultured hippocampal preparations and acute hippocampal slices. Presynaptic afferent stimulation to generate the EPSP is paired with BAPs during current clamp. The advantage of this type of protocol is that it allows for precise control of the timing between presynaptic and postsynaptic depolarization and selection of the pathway between two neurons in the hippocampus. However, the main disadvantage is that cultured hippocampal preparations

and hippocampal slices deviate from the physiological conditions in an intact hippocampal network. Hippocampal connections in a transverse plane are disconnected as are the connections within the horizontal plane to prevent back firing.

Although the technique of this STDP protocol may not have as much precision in timing of the excitation and spike as *in vitro* studies, this study offers the advantage and novelty of studying STDP *in vivo.* This study investigates the predictions of pre- and postsynaptic STDP models in a more physiologically relevant system, which includes an intact hippocampus and neural network and as such, the current rules of STDP may not apply. This study also differs from previous *in vitro* studies in location. The CA1 basal dendrites are studied rather than the apical dendrites, which are commonly studied. This will give insight to the synaptic plasticity properties of the less commonly studied dendritic tree of CA1 pyramidal neurons. Another difference is the use of a modified form of the backpropagated spike. Instead of injecting current into the soma to generate an AP that propagates back into the dendrites, a dendritic PS is generated from high intensity stimulation to the opposite dendrite (apical), which then backpropagates past the cell body and finally invades the basal dendrites. Using a protocol that more closely resembles physiological conditions *in vivo* could complicate the rules for synaptic plasticity, but would further the understanding of the mechanisms behind STDP.

4.1 Optimal Timing for Basal ES-Pairing Induced LTP

The major result from the STDP study in the basal dendrites was that all groups (-10, 0, +10, and +20 ES Interval) except for -20 ES Interval resulted in LTP of the basal excitatory sink compared to control conditions. No LTD was observed in any of the negative ES-Pairing groups. This contrasts with previous studies on STDP *in vitro* (Bi & Poo, 1998; Debanne et al., 1998; Magee & Johnston, 1997; Markham et al., 1997) that demonstrated that negative spike timing resulted in LTD. The present results are consistent with previous STDP models in that LTP was induced within a 20 ms window of positive ES Interval between the presynaptic and postsynaptic response. The present study showed that LTP was induced with either negative or positive time window, but LTP was larger at positive than negative ES Intervals (**Fig. 9**).

The BAP is suggested to be a main mechanism for LTP at positive ES time intervals. The BAP releases NMDARs from Mg^{2+} block when it occurs soon after the presynaptic excitation (Kampa et al., 2004). The high-intensity excitation of the apical dendrites generates a spike that backpropagated to the basal dendrites, and the active basal dendritic sink of the PS was detectable at ~50 to 100 μm from the cell layer. However, during ES-Pairing, the basal dendritic spike was observed to be much larger and backpropagated further (data not shown). The first 10 of the 50 ES pairs resulted in a larger basal dendritic sink that could be detected further from the cell layer, suggesting that the spike backpropagated more strongly and more distally into the basal dendrites. This observation would support the findings by Magee & Johnston (1997) and Watanabe et al. (2002) who showed that boosting of the BAPs are important for LTP. The boosting

of the BAP can be derived from the EPSP that depolarizes the dendrites, and the inactivation of A-type K^+ channels (Hoffman et al., 1997), resulting in an increase of Ca^{2+} influx through VDCCs (Bi & Poo, 1998; Froemke et al., 2006; Magee & Johnston, 1997).

The mechanism of potentiation with negative ES-Pairing groups (LTP at -10 ms ES interval and STP at -20 ES Interval) is more difficult to account for. It is possible that depolarizing afterpotential (Liu and Leung, 2004; Yue et al., 2005) may remain at the basal dendrites at 10-20 ms after a spike. However, because of the large inhibition *in vivo*, it is more likely that $GABA_A$ receptor-mediated inhibition occurs 10-20 ms after a PS, and this inhibition shunts the DAP. There may also be an involvement of metabotropic glutamate receptors (mGluRs) in LTP. High intensity stimulation may activate mGluRs leading to a release of Ca^{2+} from intracellular stores (Neyman and Manahan-Vaughan, 2008). Although purely speculative, a long-lasting means of releasing internal Ca^{2+} may potentiate the subsequent excitatory response. Future studies are necessary to identify the factors underlying LTP at both positive and negative ES Intervals.

No LTD was observed with negative ES-Pairing (-20 and -10 ES Interval) in the basal dendrites, which is contrary to STDP studies *in vitro*. A lack of precision in the ES Interval in the present experiment may explain LTP in the -10 ES Interval group. In this experiment, the maximal peak of the spike was timed according to the maximal peak of the excitatory sink. Because the excitation and the spike occur both in a population of neurons, there is some dispersion in time in the onset and peak of the excitatory sink of

individual neurons, accounting for ~2-3 ms dispersion of each event. As a result, a smaller fraction of pyramidal cells may receive excitatory input almost synchronous with the spike depolarization at the basal dendrites. Dispersion of neuronal excitation or spike is difficult to account for the STP observed with -20 ES Interval.

The -20 ES Interval group showed some STP for 10-15 minutes, which returned back to baseline at 20 min. Since many *in vitro* studies show that -20 ES-Pairing induces LTD, a major question is why LTD was not observed in the present experiment, as was observed in other experiments *in vitro*. The reasons can only be speculated. Firstly, the pathway being studied in this experiment is different from those in the *in vitro* studies. As explained below, as compared to other synapses and other cells, the basal dendrites of CA1 pyramidal cells may be prone to LTP and not LTD on account of electrotonic properties and NMDA receptors.

4.2 Difference Between Basal and Apical Dendrites

It has been shown for some time that LTP is much easier to generate in the basal dendrites compared to the apical dendrites (Arai et al., 1994; Capocchi et al., 1992; Leung et al., 1992; Kaibara and Leung, 1993; Leung and Shen, 1995; Roth and Leung, 1995). The basal dendrites have a lower threshold for LTP *in vivo* and can potentiate easier with lower frequency bursts of theta rhythm, while the apical usually require activation by higher stimulation frequencies for LTP induction (Kaibara and Leung, 1993; Leung and Shen, 1995). One suggestion for this difference in the properties

between the basal and apical dendrites in CA1 is due to differential effects of inhibitory cells across dendritic subfields (Arai et al., 1994; Kaibara and Leung, 1993). A specific synaptic plasticity induction protocol, theta-frequency primed-burst stimulation, may be more effective in activating the interneurons in the apical (Lacaille et al., 1988) versus basal (Lacaille et al., 1987) dendrites (Roth and Leung, 1995).

The reasons for the lack of LTD with negative ES Interval may be due to the properties of the basal dendrites themselves. One reason may be the relative lack of inhibition at the basal dendrites. As compared to the apical dendrites, CA1 pyramidal cells have basal dendrites that are shorter and less branched (Ishizuka et al., 1995), which would allow for less electrotonic attenuation (Henze et al., 1996) and higher depolarization levels for a given current. A higher depolarization would allow the BAPs to open more VDCCs (Christie et al., 1995; Jaffe et al., 1992) and more NMDAR channels. Also, there could be a higher density of VDCCs in the basal dendritic region compared to the apical dendritic regions (Cavus and Teyler, 1998). In the basal dendrites of neocortical layer 5 pyramidal cells, BAPs have been shown to evoke the largest Ca^{2+} accumulation (Schiller et al., 1995) and induced NMDAR mediated spikes (Schiller et al., 2001). The relative ease with which the basal dendrites can exhibit LTP may explain the results found in negative ES-Pairing in the basal dendrites and also coincident ES-Pairing in the apical dendrites. The High Basal Stimulation Only group, which involved high-intensity stimulation to the basal dendrites, and the 0 ES Interval group showed potentiation of the basal excitatory sink even though ES-Pairing was not occurring in that region. In comparison, the High Apical Stimulation Only group, which involved high-intensity stimulation to the apical dendrites, did not result in potentiation of the apical

excitatory sink. Thus, it may be that the basal dendrites are more susceptible to LTP and are unable to exhibit LTD.

In this study, we reproduced the results of Thiels et al. (1994) that 150-200 paired pulse stimulations at 0.5 Hz and high-intensity induced LTD of up to 2 h in the apical dendrites of CA1 *in vivo*. The first stimulus generated a PS, followed by inhibition of the PS evoked by the second stimulus given 25 ms later. This protocol is very similar to negative ES-Pairing because there is a 25 ms delay between the PS and the excitatory sink. However, the difference is that this protocol involves homosynaptic excitation while the ES-Pairing protocol involves heterosynaptic excitation. The LTD generated in the apical dendrites is dependent on activation of NMDARs (Thiels et al., 1994). STDP LTD has also been shown to be NMDAR dependent (reviewed by Caporale and Dan, 2008). However, the same protocol of high-intensity paired-pulse stimulation at 25 ms interval given to the basal dendrites did not induce LTD. This suggests that the properties of the NMDA receptor may be different between the apical and the basal dendrites.

The NMDAR is composed of hetero-oligomer subunits (NR1, NR2, and occasionally NR3) (Cull-Candy et al., 2001). They require two obligatory NR1 subunits and two regulatory subunits that can be NR2 or NR3. The NR2 subunit family has four distinct subtypes (NR2A-D). The NR2A and NR2B subunits mostly dominate the rat hippocampus (Watanabe et al., 1993; Monyer et al., 1994; Wenzel et al., 1995; Dunah et al., 1996; Fritschy et al., 1998). The NMDAR subunits have been implicated in determining the direction of synaptic plasticity changes; it has been shown that NR2A is

important for LTD, while NR2B is important for LTP (reviewed by Yashiro and Philpot, 2008).

NR2B-containing NMDA receptors have been shown to reveal longer currents (Monyer et al., 1994) and interact with CamKII compared to NR2A-containing NMDARs (Strack and Colbran, 1998). Many studies in the hippocampus support the hypothesis that NR2B is involved in LTP because NMDARs containing these subunits have been shown to recruit a larger influx of Ca^{2+} than NMDARs composed of NR2A subunits. Ifenprodil, an NR2B-specific antagonist, completely blocks LTP induced by a pairing protocol (Barria and Malinow, 2005). They further showed that overexpression of NR2A and replacement of NR2B with NR2A subtypes attenuates the induction of LTP by a pairing protocol. Also overexpression of NR2B enhances hippocampal LTP, while blocking NR2B and CamKII interaction inhibits LTP in mice (Tang et al., 1999; Zhou et al., 2007). Thus, it is tempting to suggest that NR2B-containing NMDARs contribute to the induction of LTP. However there is conflicting evidence that show that NR2A are important for LTP. Blocking the NR2A-containing NMDARs with NVP-AAM077 blocked LTP in 3-4 week old rats (Liu et al., 2004) and blocked LTP in adult perirhinal cortex (Liu et al., 2004; Massey et al., 2004).

In contrast, the role of NR2A's involvement in LTD is less clear than the involvement of NR2B in LTP. It has been shown that NR2B blockade by infenprodil did not affect LTD (Morishita et al., 2006), which demonstrates that induction of LTD does not require NR2B-containing-NMDARs. In the visual cortex, 1 Hz stimulation protocol (900 pulses) induced LTP in mice lacking NR2A, which normally induces LTD in wild

type mice (Philpot et al., 2007). On the other hand, 0.5 Hz stimulation at 900 pulses induces LTD in mice lacking NR2A compared to wild type. More studies need to clarify the possible role of NR2A in LTD.

Because of the conflicting results, a ratio of NR2A:NR2B has been proposed to determine the direction of synaptic plasticity. It has been speculated that synapses which possess a high NR2A/NR2B ratio would favour the induction of LTD, and synapses which possess a low NR2A/NR2B ratio would favour the induction of LTP (reviewed by Yashiro and Philpot, 2008). It has been documented that the allocation of the NR2B subunit is asymmetrical in the hippocampal circuitry of mice (Kawakami et al., 2003). CA3 afferents to CA1 pyramidal cells at both apical and basal dendrites consist of both association and commissural fibers, and the association fibers remained 5 days after transection of the ventral hippocampal commissure in mice (Kawakami et al., 2003). In these mice with transected ventral hippocampal commissures, NR2B mediated NMDA receptor response is more prevalent in the CA1 apical dendrites of the left hippocampus and in the basal dendrites of CA1 pyramidal cells of the right hippocampus. The present study used the right hippocampus of the rat, and if the NMDA receptor asymmetry in the rat is similar to that in the mouse, and if the local stimuli used evoked more associational response than commissural response, then the basal dendritic response in the present study is expected to show a high NR2B to NR2A ratio, or a higher likelihood of LTP than LTD. The same logic would predict that ES-Pairing protocol applied to the basal dendrites of CA1 pyramidal cells of the left hippocampus would preferentially show LTD and not LTP. Other than the conditional statements assumed, the dependence of

LTP/LTD on NR2A/B subunits remains to be confirmed for ES-Pairing at the basal/apical dendrites of CA1 pyramidal cells of rats.

4.3 Studying the Apical Dendrites after Basal ES-Pairing

This experiment is unique in that synaptic changes in the apical dendrites can be seen while ES-Pairing is induced in the basal dendrites. Although there was no apical dendritic LTP in the positive and negative ES-Pairing groups (-20,-10, 0, +10, +20 ES Interval) compared to the control groups, there are significant differences within each group compared to its own baseline. While only -20 and +20 ES Interval showed post-hoc differences after a one way (time) ANOVA, all 5 groups were significantly potentiated after ES-Pairing compared to baseline. This unexpected potentiation may be due to the mechanism of the dendritic spikes that we used to pair excitatory input in the basal dendrites with a spike originating from the apical dendrites. High intensity stimulation was used in the apical dendrites to create an excitation that generated a PS, which then invaded the basal dendrites. Thus, there would be simultaneous synaptic excitation and PS occurring which could involve a similar mechanism as the coincident ES-Pairing in the basal dendrites and cause potentiation of the apical dendrites. Even the control (High Apical Stimulation Only) shows some potentiation of the apical excitatory sink. Generating dendritic spikes that propagate to the opposite dendrite may be a way to facilitate LTP across both basal and apical dendrites if there were coincident presynaptic basal dendritic afferent activity. This function may be a way to associate synaptic

plasticity throughout specific CA1 pyramidal cells that receive basal and apical excitation at a particular time delay.

4.4 Studying the Apical and Basal Dendrites after Apical ES-Pairing

In the experiment studying ES-Pairing in the apical dendrites, similar results to ES-Pairing in the basal dendrites were obtained. LTP was observed in the apical dendrites after coincident (0ms) ES-Pairing compared to control conditions. The proposed mechanism for LTP, mentioned above, during STDP in the basal dendrites stemmed from STDP research in the apical dendrites. That mechanism likely explains the LTP in this case. However, ES-Pairing in the apical dendrites also caused LTP of the basal dendrites. Even the control group (High Basal Stimulation Only) resulted in potentiation of the basal excitatory sink. The potential explanation for this is mentioned above in section 5.2. Firstly, the basal dendrites are more susceptible to LTP than the apical dendrites, which may explain the LTP. Also, the same result occurred during ES-Pairing in the basal dendrites; the apical sink showed potentiation after ES-Pairing at all time delays within the groups. Again, the simultaneous excitation and the generation of the spike are coincident and may employ similar mechanisms for STDP LTP as the opposite dendrites which are receiving the ES-Pairing. Future experiments need to expand on these current studies and test negative and positive ES-Pairing in the apical dendrites. Showing STDP LTD in the apical dendrites using the same protocol in this experiment would support the theory that the dendritic properties of the basal dendrites are inherently different from the apical dendrites.

4.5 The Importance of Spike Timing

The time window of 20 ms may be relevant *in vivo*. According to Yeckel and Berger (1998), the latencies to responses in the trisynaptic pathway following medial perforant path (output of entorhinal cortex) stimulation in the anesthetized rabbit were as follows: DG cells, 4.5-5.5 ms; disynaptic excitation of CA3, 8-13 ms; and trisynaptic excitation of CA1, 16-21 ms. Latencies of medial perforant path excitation of CA1 and CA3 in the anesthetized rat were somewhat shorter, with monosynaptic excitation at 5-8 ms in CA1 (Leung et al., 1995), and ~5-6 ms in CA3a (Fung et al., 2011). The 5-6 ms delay plus the 4-6 ms monosynaptic delay for the response of CA1 cells evoked by the Schaffer collateral stimulation (Roth and Leung, 1995) would result in a total disynaptic latency of 9-12 ms, and the trisynaptic excitation latency 4-6 ms later. Thus, mono-, di- and tri-synaptic excitation of CA1 are within 15 ms. Two pathways, one through the disynaptic pathway and one through the trisynaptic pathway to CA1 would result in two signals arriving within 5 ms or less within each other. Also, it would be expected that excitation through a monosynaptic pathway and a trisynaptic pathway to CA1 would result in a delay of the two signals that is greater than 10 ms. Therefore, due to the different excitatory innervations of the basal and apical dendrites in CA1, there may be a physiological relevance of STDP because impulses will arrive at the same dendrite in CA1 pyramidal neurons within a 20 ms time window.

Since the introduction of the Hebbian synapse in 1949, the concepts underlying synaptic plasticity have advanced dramatically. The first big step for STDP was the full characterization of the timing window for the induction of synaptic plasticity using pairs

of single presynaptic and postsynaptic action potentials by Bi and Poo (1998) and Debanne et al. (1998) in the hippocampus. They used cultured hippocampal preparations, which allowed pairs of connected cells to be recorded easily and allowed for precise control of the spiking of both pre- and post-synaptic neurons. However, the drawback of hippocampal cultures is the divergence of culture conditions from an intact hippocampal network. Another disadvantage is that with slice cultures, it is unclear what developmental stage the cultured network represented (Buchanan and Mellor, 2010). Since then, many groups began to take an interest in studying this elegant model for plasticity induction moving toward more *in vivo* like conditions. Groups began to investigate STDP timing curves in acute hippocampal slices pairing extracellular Schaffer collateral stimulation with APs generated in patched CA1 pyramidal cells. For example, Nishiyama et al. (2000) reported similar STDP curve observed by Bi and Poo, when they paired Schaffer collateral stimulation with single post-synaptic spikes in hippocampal slices in young adult rats. However, many groups have been unable to induce STDP with single postsynaptic spikes. Instead they used pairs of Schaffer collateral stimulations with bursts of postsynaptic APs to induce LTP in acute hippocampal slices (Pike et al., 1999; Watanabe et al., 2002; Meredith et al., 2003; Wittenberg and Wang, 2006; Buchanan and Mellor, 2007; Carlisle et al., 2008).

The move towards more *in vivo* conditions has complicated spike timing in the hippocampus. The timing dependence of presynaptic spikes and postsynaptic burst firing in the acute hippocampal slices have only been reported from immature animals, which have produced a variety of inconsistent results. Pairs of single presynaptic and postsynaptic spikes given at positive timing intervals have induced either; no plasticity

(Buchanan and Mellor, 2007), LTD (Wittenberg and Wang, 2006; Campanac and Debanne, 2008) or LTP (Meredith et al., 2003; Buchanan and Mellor, 2007; Campanac and Debanne, 2008) dependent on specific experimental conditions. These inconsistencies have resulted in many groups moving towards studying STDP on synapses in the neocortex because of the relative ease in obtaining paired electrophysiological recordings from synaptically coupled neurons in cortical slices. Several *in vivo* studies on STDP have emerged recently illustrating STDP using electrical stimulation (Jacob et al., 2006; Zhang et al., 1998), sensory stimulation (Fu et al., 2002; Yao et al., 2004), and motion stimulation (Fu et al., 2004) in cortical neurons. However, few to our knowledge have studied STDP *in vivo* in the hippocampus.

This study is one of the first to study STDP *in vivo* in the hippocampus revisiting the original and simple STDP model used by Bi and Poo in 1998. Major differences between this and previous studies are the use of a different pathway that studies the basal dendrites as opposed to the apical dendrites of CA1 pyramidal cells, the use of a backpropagating dendritic spike, and the ability to observe both the basal and apical dendrites while ES-Pairing in either region. This study also differs from other *in vivo* studies such that the stimulation and timing are finely controlled compared to sensory or motion stimuli which may be quite variable. Although this study was only able to show STDP LTP and not LTD, which is inconsistent with Bi and Poo's observations, the plasticity observed is still dependent on the coincident of presynaptic and postsynaptic activity as excitatory sinks or postsynaptic PS given on their own fail to induce plasticity. Also, a timing window to generate LTP is still observed. This study helps to further the understanding of the Hebbian synapse. The results obtained in this study will contribute

to the common underlying theme that is starting to unveil a clearer picture of STDP rules in the hippocampus.

4.6 Conclusion

In this study, ES-Pairing at the hippocampal CA1 basal dendrites revealed a time window to induce synaptic plasticity. ES-Pairing at all positive time intervals studied (0-20 ms) resulted in LTP. ES-Pairing at a negative time interval also resulted in LTP, but only at -10 ms (postsynaptic EPSP preceded the spike by 10 ms). Furthermore, ES-Pairing at the basal dendrites resulted in some potentiation in the apical dendrites. The potentiation that occurs on both sides of the dendrites may be a way to associate synaptic plasticity throughout specific CA1 cells that receive both basal and apical excitation at a particular time delay. In addition, the homosynaptic paired pulse protocol induced LTD in the apical dendrites of CA1, but did not induce LTD when given to the basal dendrites. Thus, it is suggested that there may be a difference in the properties of NMDA receptors between the basal and apical dendrites, with the basal dendrites favouring LTP. Finally, coincident ES-Pairing in the apical dendrites resulted in LTP of the apical dendrites and the basal dendrites.

5. REFERENCES

Abbott, L.F., and Nelson, S.B. (2000). Synaptic plasticity: taming the beast. Nat. Neurosci. 3 Suppl, 1178-1183.

Abraham, W.C., Gustafsson, B., and Wigstrom, H. (1986). Single high strength afferent volleys can produce long-term potentiation in the hippocampus in vitro. Neurosci. Lett. 70, 217-222.

Amaral, D.G., and Witter, M.P. (1989). The three-dimensional organization of the hippocampal formation: a review of anatomical data. Neuroscience 31, 571-591.

Anderson, P., Bliss, T.V., and Skrede, K.K. (1971). Lamellar organization of hippocampal pathways. Exp. Brain Res. 13, 222-238.

Arai, A., Black, J., and Lynch, G. (1994). Origins of the variations in long-term potentiation between synapses in the basal versus apical dendrites of hippocampal neurons. Hippocampus 4, 1-9.

Ascher, P., and Nowak, L. (1988). The role of divalent cations in the N-methyl-D-aspartate responses of mouse central neurones in culture. J. Physiol. 399, 247-266.

Augustine, G.J., Fitzpatrick, D., Hall, W.C., LaMantia, A., McNamara, J.O., Mooney, R.D., Platt, M.L., Purves, D., Simon, S.A., White, L.E., and Williams, S.M. (2007). The Changing Brain. In Neuroscience, Sinauer Associates, Inc.)

Barria, A., Derkach, V., and Soderling, T. (1997). Identification of the Ca2+/calmodulin-dependent protein kinase II regulatory phosphorylation site in the alpha-amino-3-hydroxyl-5-methyl-4-isoxazole-propionate-type glutamate receptor. J. Biol. Chem. 272, 32727-32730.

Barria, A., and Malinow, R. (2005). NMDA receptor subunit composition controls synaptic plasticity by regulating binding to CaMKII. Neuron 48, 289-301.

Bender, V.A., Bender, K.J., Brasier, D.J., and Feldman, D.E. (2006). Two coincidence detectors for spike timing-dependent plasticity in somatosensory cortex. J. Neurosci. 26, 4166-4177.

Benke, T.A., Luthi, A., Isaac, J.T., and Collingridge, G.L. (1998). Modulation of AMPA receptor unitary conductance by synaptic activity. Nature 393, 793-797.

Bi, G.Q., and Poo, M.M. (1998). Synaptic modifications in cultured hippocampal neurons: dependence on spike timing, synaptic strength, and postsynaptic cell type. J. Neurosci. 18, 10464-10472.

Bliss, T.V., and Lomo, T. (1973). Long-lasting potentiation of synaptic transmission in the dentate area of the anaesthetized rabbit following stimulation of the perforant path. J. Physiol. 232, 331-356.

Boettiger, C.A., and Doupe, A.J. (2001). Developmentally restricted synaptic plasticity in a songbird nucleus required for song learning. Neuron 31, 809-818.

Bredt, D.S., and Nicoll, R.A. (2003). AMPA receptor trafficking at excitatory synapses. Neuron 40, 361-379.

Buchanan, K.A., and Mellor, J.R. (2010). The activity requirements for spike timing-dependent plasticity in the hippocampus. Front. Synaptic Neurosci. 2, 11.

Buchanan, K.A., and Mellor, J.R. (2007). The development of synaptic plasticity induction rules and the requirement for postsynaptic spikes in rat hippocampal CA1 pyramidal neurones. J. Physiol. 585, 429-445.

Campanac, E., and Debanne, D. (2008). Spike timing-dependent plasticity: a learning rule for dendritic integration in rat CA1 pyramidal neurons. J. Physiol. 586, 779-793.

Capocchi, G., Zampolini, M., and Larson, J. (1992). Theta burst stimulation is optimal for induction of LTP at both apical and basal dendritic synapses on hippocampal CA1 neurons. Brain Res. 591, 332-336.

Caporale, N., and Dan, Y. (2008). Spike timing-dependent plasticity: a Hebbian learning rule. Annu. Rev. Neurosci. 31, 25-46.

Cassenaer, S., and Laurent, G. (2007). Hebbian STDP in mushroom bodies facilitates the synchronous flow of olfactory information in locusts. Nature 448, 709-713.

Cavus, I., and Teyler, T. (1996). Two forms of long-term potentiation in area CA1 activate different signal transduction cascades. J. Neurophysiol. 76, 3038-3047.

Cavus, I., and Teyler, T.J. (1998). NMDA receptor-independent LTP in basal versus apical dendrites of CA1 pyramidal cells in rat hippocampal slice. Hippocampus 8, 373-379.

Christie, B.R., Eliot, L.S., Ito, K., Miyakawa, H., and Johnston, D. (1995). Different Ca2+ channels in soma and dendrites of hippocampal pyramidal neurons mediate spike-induced Ca2+ influx. J. Neurophysiol. 73, 2553-2557.

Citri, A., and Malenka, R.C. (2008). Synaptic plasticity: multiple forms, functions, and mechanisms. Neuropsychopharmacology 33, 18-41.

Collingridge, G.L., Kehl, S.J., and McLennan, H. (1983). Excitatory amino acids in synaptic transmission in the Schaffer collateral-commissural pathway of the rat hippocampus. J. Physiol. 334, 33-46.

Cull-Candy, S., Brickley, S., and Farrant, M. (2001). NMDA receptor subunits: diversity, development and disease. Curr. Opin. Neurobiol. 11, 327-335.

Dan, Y., and Poo, M.M. (2006). Spike timing-dependent plasticity: from synapse to perception. Physiol. Rev. 86, 1033-1048.

Davies, C.H., Starkey, S.J., Pozza, M.F., and Collingridge, G.L. (1991). GABA autoreceptors regulate the induction of LTP. Nature 349, 609-611.

Debanne, D., Gahwiler, B.H., and Thompson, S.M. (1998). Long-term synaptic plasticity between pairs of individual CA3 pyramidal cells in rat hippocampal slice cultures. J. Physiol. 507 (Pt 1), 237-247.

Debanne, D., Gahwiler, B.H., and Thompson, S.M. (1996). Cooperative interactions in the induction of long-term potentiation and depression of synaptic excitation between hippocampal CA3-CA1 cell pairs in vitro. Proc. Natl. Acad. Sci. U. S. A. 93, 11225-11230.

Derkach, V.A., Oh, M.C., Guire, E.S., and Soderling, T.R. (2007). Regulatory mechanisms of AMPA receptors in synaptic plasticity. Nat. Rev. Neurosci. 8, 101-113.

Destexhe, A., Rudolph, M., and Pare, D. (2003). The high-conductance state of neocortical neurons in vivo. Nat. Rev. Neurosci. 4, 739-751.

Diamond, D.M., Dunwiddie, T.V., and Rose, G.M. (1988). Characteristics of hippocampal primed burst potentiation in vitro and in the awake rat. J. Neurosci. 8, 4079-4088.

Douglas, R.M., and Goddard, G.V. (1975). Long-term potentiation of the perforant path-granule cell synapse in the rat hippocampus. Brain Res. 86, 205-215.

Dunah, A.W., Yasuda, R.P., Wang, Y.H., Luo, J., Davila-Garcia, M., Gbadegesin, M., Vicini, S., and Wolfe, B.B. (1996). Regional and ontogenic expression of the NMDA receptor subunit NR2D protein in rat brain using a subunit-specific antibody. J. Neurochem. 67, 2335-2345.

Egger, V., Feldmeyer, D., and Sakmann, B. (1999). Coincidence detection and changes of synaptic efficacy in spiny stellate neurons in rat barrel cortex. Nat. Neurosci. 2, 1098-1105.

Feldman, D.E. (2000). Timing-based LTP and LTD at vertical inputs to layer II/III pyramidal cells in rat barrel cortex. Neuron 27, 45-56.

Freeman, J.A., and Nicholson, C. (1975). Experimental optimization of current source-density technique for anuran cerebellum. J. Neurophysiol. 38, 369-382.

Frey, U., Huang, Y.Y., and Kandel, E.R. (1993). Effects of cAMP simulate a late stage of LTP in hippocampal CA1 neurons. Science 260, 1661-1664.

Fritschy, J.M., Weinmann, O., Wenzel, A., and Benke, D. (1998). Synapse-specific localization of NMDA and GABA(A) receptor subunits revealed by antigen-retrieval immunohistochemistry. J. Comp. Neurol. 390, 194-210.

Froemke, R.C., and Dan, Y. (2002). Spike-timing-dependent synaptic modification induced by natural spike trains. Nature 416, 433-438.

Froemke, R.C., Poo, M.M., and Dan, Y. (2005). Spike-timing-dependent synaptic plasticity depends on dendritic location. Nature 434, 221-225.

Froemke, R.C., Tsay, I.A., Raad, M., Long, J.D., and Dan, Y. (2006). Contribution of individual spikes in burst-induced long-term synaptic modification. J. Neurophysiol. 95, 1620-1629.

Fu, Y.X., Djupsund, K., Gao, H., Hayden, B., Shen, K., and Dan, Y. (2002). Temporal specificity in the cortical plasticity of visual space representation. Science 296, 1999-2003.

Fu, Y.X., Shen, Y., Gao, H., and Dan, Y. (2004). Asymmetry in visual cortical circuits underlying motion-induced perceptual mislocalization. J. Neurosci. 24, 2165-2171.

Fukunaga, K., Muller, D., and Miyamoto, E. (1995). Increased phosphorylation of Ca2+/calmodulin-dependent protein kinase II and its endogenous substrates in the induction of long-term potentiation. J. Biol. Chem. 270, 6119-6124.

Fung, T.K., Peloquin, P., Wu, K., and Leung, L.S. (2011). Differential long-term depression in CA3 but not in dentate gyrus following low-frequency stimulation of the medial perforant path. Synapse 65, 677-686.

Harvey, J., and Collingridge, G.L. (1992). Thapsigargin blocks the induction of long-term potentiation in rat hippocampal slices. Neurosci. Lett. 139, 197-200.

Hebb, D.O. The Organization of Behavior. New York: Wiley

Henze, D.A., Cameron, W.E., and Barrionuevo, G. (1996). Dendritic morphology and its effects on the amplitude and rise-time of synaptic signals in hippocampal CA3 pyramidal cells. J. Comp. Neurol. 369, 331-344.

Hoffman, D.A., Magee, J.C., Colbert, C.M., and Johnston, D. (1997). K+ channel regulation of signal propagation in dendrites of hippocampal pyramidal neurons. Nature 387, 869-875.

Isaacson, R.L. (1980). A perspective for the interpretation of limbic system function. Physiology and Psychology 8, 183-188.

Ishizuka, N., Cowan, W.M., and Amaral, D.G. (1995). A quantitative analysis of the dendritic organization of pyramidal cells in the rat hippocampus. J. Comp. Neurol. 362, 17-45.

Ishizuka, N., Weber, J., and Amaral, D.G. (1990). Organization of intrahippocampal projections originating from CA3 pyramidal cells in the rat. J. Comp. Neurol. 295, 580-623.

Jacob, V., Brasier, D.J., Erchova, I., Feldman, D., and Shulz, D.E. (2007). Spike timing-dependent synaptic depression in the in vivo barrel cortex of the rat. J. Neurosci. 27, 1271-1284.

Jaffe, D.B., Johnston, D., Lasser-Ross, N., Lisman, J.E., Miyakawa, H., and Ross, W.N. (1992). The spread of Na+ spikes determines the pattern of dendritic Ca2+ entry into hippocampal neurons. Nature 357, 244-246.

Jahr, C.E., and Stevens, C.F. (1987). Glutamate activates multiple single channel conductances in hippocampal neurons. Nature 325, 522-525.

Kaibara, T., and Leung, L.S. (1993). Basal versus apical dendritic long-term potentiation of commissural afferents to hippocampal CA1: a current-source density study. J. Neurosci. 13, 2391-2404.

Kampa, B.M., Clements, J., Jonas, P., and Stuart, G.J. (2004). Kinetics of Mg2+ unblock of NMDA receptors: implications for spike-timing dependent synaptic plasticity. J. Physiol. 556, 337-345.

Kawakami, R., Shinohara, Y., Kato, Y., Sugiyama, H., Shigemoto, R., and Ito, I. (2003). Asymmetrical allocation of NMDA receptor epsilon2 subunits in hippocampal circuitry. Science 300, 990-994.

Kloosterman, F., Peloquin, P., and Leung, L.S. (2001). Apical and basal orthodromic population spikes in hippocampal CA1 in vivo show different origins and patterns of propagation. J. Neurophysiol. 86, 2435-2444.

Knowles, W.D. (1992). Normal anatomy and neurophysiology of the hippocampal formation. J. Clin. Neurophysiol. 9, 252-263.

Koester, H.J., and Sakmann, B. (1998). Calcium dynamics in single spines during coincident pre- and postsynaptic activity depend on relative timing of back-propagating action potentials and subthreshold excitatory postsynaptic potentials. Proc. Natl. Acad. Sci. U. S. A. 95, 9596-9601.

Kramar, E.A., and Lynch, G. (2003). Developmental and regional differences in the consolidation of long-term potentiation. Neuroscience 118, 387-398.

Lacaille, J.C., Mueller, A.L., Kunkel, D.D., and Schwartzkroin, P.A. (1987). Local circuit interactions between oriens/alveus interneurons and CA1 pyramidal cells in hippocampal slices: electrophysiology and morphology. J. Neurosci. 7, 1979-1993.

Lacaille, J.C., and Schwartzkroin, P.A. (1988). Stratum lacunosum-moleculare interneurons of hippocampal CA1 region. II. Intrasomatic and intradendritic recordings of local circuit synaptic interactions. J. Neurosci. 8, 1411-1424.

Lester, R.A., Clements, J.D., Westbrook, G.L., and Jahr, C.E. (1990). Channel kinetics determine the time course of NMDA receptor-mediated synaptic currents. Nature 346, 565-567.

Leung, L.S., and Peloquin, P. (2010). Cholinergic modulation differs between basal and apical dendritic excitation of hippocampal CA1 pyramidal cells. Cereb. Cortex 20, 1865-1877.

Leung, L.S., Roth, L., and Canning, K.J. (1995). Entorhinal inputs to hippocampal CA1 and dentate gyrus in the rat: a current-source-density study. J. Neurophysiol. 73, 2392-2403.

Leung, L.S., and Shen, B. (1995). Long-term potentiation at the apical and basal dendritic synapses of CA1 after local stimulation in behaving rats. J. Neurophysiol. 73, 1938-1946.

Leung, L.S., Shen, B., and Kaibara, T. (1992). Long-term potentiation induced by patterned stimulation of the commissural pathway to hippocampal CA1 region in freely moving rats. Neuroscience 48, 63-74.

Leung, L.W. (1979). Orthodromic activation of hippocampal CA1 region of the rat. Brain Res. 176, 49-63.

Leung, L.S. (2010). Field potential generation and current source density analysis. In: Electrophysiological Recording Techniques. Vertes, R.P. and Stackman, R.W. (Eds.),. Clifton, N.J.: Humana Press. NeuroMethods, Volume 15:1-26.

Levy, W.B., and Steward, O. (1983). Temporal contiguity requirements for long-term associative potentiation/depression in the hippocampus. Neuroscience 8, 791-797.

Li, X.G., Somogyi, P., Ylinen, A., and Buzsaki, G. (1994). The hippocampal CA3 network: an in vivo intracellular labeling study. J. Comp. Neurol. 339, 181-208.

Liu, L., Wong, T.P., Pozza, M.F., Lingenhoehl, K., Wang, Y., Sheng, M., Auberson, Y.P., and Wang, Y.T. (2004). Role of NMDA receptor subtypes in governing the direction of hippocampal synaptic plasticity. Science 304, 1021-1024.

Liu, X., and Stan Leung, L. (2004). Sodium-activated potassium conductance participates in the depolarizing afterpotential following a single action potential in rat hippocampal CA1 pyramidal cells. Brain Res. 1023, 185-192.

Lynch, G., Larson, J., Kelso, S., Barrionuevo, G., and Schottler, F. (1983). Intracellular injections of EGTA block induction of hippocampal long-term potentiation. Nature 305, 719-721.

MacDermott, A.B., Mayer, M.L., Westbrook, G.L., Smith, S.J., and Barker, J.L. (1986). NMDA-receptor activation increases cytoplasmic calcium concentration in cultured spinal cord neurones. Nature 321, 519-522.

Magee, J.C., and Johnston, D. (1997). A synaptically controlled, associative signal for Hebbian plasticity in hippocampal neurons. Science 275, 209-213.

Malenka, R.C., and Bear, M.F. (2004). LTP and LTD: an embarrassment of riches. Neuron 44, 5-21.

Malenka, R.C., Kauer, J.A., Perkel, D.J., Mauk, M.D., Kelly, P.T., Nicoll, R.A., and Waxham, M.N. (1989). An essential role for postsynaptic calmodulin and protein kinase activity in long-term potentiation. Nature 340, 554-557.

Malenka, R.C., and Nicoll, R.A. (1999). Long-term potentiation--a decade of progress? Science 285, 1870-1874.

Malinow, R., and Malenka, R.C. (2002). AMPA receptor trafficking and synaptic plasticity. Annu. Rev. Neurosci. 25, 103-126.

Malinow, R., Schulman, H., and Tsien, R.W. (1989). Inhibition of postsynaptic PKC or CaMKII blocks induction but not expression of LTP. Science 245, 862-866.

Markram, H., Lubke, J., Frotscher, M., and Sakmann, B. (1997). Regulation of synaptic efficacy by coincidence of postsynaptic APs and EPSPs. Science 275, 213-215.

Massey, P.V., Johnson, B.E., Moult, P.R., Auberson, Y.P., Brown, M.W., Molnar, E., Collingridge, G.L., and Bashir, Z.I. (2004). Differential roles of NR2A and NR2B-containing NMDA receptors in cortical long-term potentiation and long-term depression. J. Neurosci. 24, 7821-7828.

Mayer, M.L., Westbrook, G.L., and Guthrie, P.B. (1984). Voltage-dependent block by Mg2+ of NMDA responses in spinal cord neurones. Nature 309, 261-263.

Megias, M., Emri, Z., Freund, T.F., and Gulyas, A.I. (2001). Total number and distribution of inhibitory and excitatory synapses on hippocampal CA1 pyramidal cells. Neuroscience 102, 527-540.

Meredith, R.M., Floyer-Lea, A.M., and Paulsen, O. (2003). Maturation of long-term potentiation induction rules in rodent hippocampus: role of GABAergic inhibition. J. Neurosci. 23, 11142-11146.

Montgomery, J.M., Pavlidis, P., and Madison, D.V. (2001). Pair recordings reveal all-silent synaptic connections and the postsynaptic expression of long-term potentiation. Neuron 29, 691-701.

Monyer, H., Burnashev, N., Laurie, D.J., Sakmann, B., and Seeburg, P.H. (1994). Developmental and regional expression in the rat brain and functional properties of four NMDA receptors. Neuron 12, 529-540.

Morgane, P.J., Galler, J.R., and Mokler, D.J. (2005). A review of systems and networks of the limbic forebrain/limbic midbrain. Prog. Neurobiol. 75, 143-160.

Morishita, W., Lu, W., Smith, G.B., Nicoll, R.A., Bear, M.F., and Malenka, R.C. (2007). Activation of NR2B-containing NMDA receptors is not required for NMDA receptor-dependent long-term depression. Neuropharmacology 52, 71-76.

Nevian, T., and Sakmann, B. (2006). Spine Ca2+ signaling in spike-timing-dependent plasticity. J. Neurosci. 26, 11001-11013.

Nevian, T., and Sakmann, B. (2004). Single spine Ca2+ signals evoked by coincident EPSPs and backpropagating action potentials in spiny stellate cells of layer 4 in the juvenile rat somatosensory barrel cortex. J. Neurosci. 24, 1689-1699.

Neyman, S., and Manahan-Vaughan, D. (2008). Metabotropic glutamate receptor 1 (mGluR1) and 5 (mGluR5) regulate late phases of LTP and LTD in the hippocampal CA1 region in vitro. Eur. J. Neurosci. 27, 1345-1352.

Nishiyama, M., Hong, K., Mikoshiba, K., Poo, M.M., and Kato, K. (2000). Calcium stores regulate the polarity and input specificity of synaptic modification. Nature 408, 584-588.

Nowak, L., Bregestovski, P., Ascher, P., Herbet, A., and Prochiantz, A. (1984). Magnesium gates glutamate-activated channels in mouse central neurones. Nature 307, 462-465.

Park, M., Penick, E.C., Edwards, J.G., Kauer, J.A., and Ehlers, M.D. (2004). Recycling endosomes supply AMPA receptors for LTP. Science 305, 1972-1975.

Paxinos G., W.C. (1986). The Rat Brain in Stereotaxic Coordinates

Philpot, B.D., Cho, K.K., and Bear, M.F. (2007). Obligatory role of NR2A for metaplasticity in visual cortex. Neuron 53, 495-502.

Pike, F.G., Meredith, R.M., Olding, A.W., and Paulsen, O. (1999). Rapid report: postsynaptic bursting is essential for 'Hebbian' induction of associative long-term potentiation at excitatory synapses in rat hippocampus. J. Physiol. 518 (Pt 2), 571-576.

Pyapali, G.K., Sik, A., Penttonen, M., Buzsaki, G., and Turner, D.A. (1998). Dendritic properties of hippocampal CA1 pyramidal neurons in the rat: intracellular staining in vivo and in vitro. J. Comp. Neurol. 391, 335-352.

Rose, G.M., and Dunwiddie, T.V. (1986). Induction of hippocampal long-term potentiation using physiologically patterned stimulation. Neurosci. Lett. 69, 244-248.

Rosenmund, C., Feltz, A., and Westbrook, G.L. (1995). Calcium-dependent inactivation of synaptic NMDA receptors in hippocampal neurons. J. Neurophysiol. 73, 427-430.

Roth, L.R., and Leung, L.S. (1995). Difference in LTP at basal and apical dendrites of CA1 pyramidal neurons in urethane-anesthetized rats. Brain Res. 694, 40-48.

Schiller, J., Helmchen, F., and Sakmann, B. (1995). Spatial profile of dendritic calcium transients evoked by action potentials in rat neocortical pyramidal neurones. J. Physiol. 487 (Pt 3), 583-600.

Schiller, J., Major, G., Koester, H.J., and Schiller, Y. (2000). NMDA spikes in basal dendrites of cortical pyramidal neurons. Nature 404, 285-289.

Silva, A.J., Stevens, C.F., Tonegawa, S., and Wang, Y. (1992). Deficient hippocampal long-term potentiation in alpha-calcium-calmodulin kinase II mutant mice. Science 257, 201-206.

Sjostrom, P.J., Turrigiano, G.G., and Nelson, S.B. (2001). Rate, timing, and cooperativity jointly determine cortical synaptic plasticity. Neuron 32, 1149-1164.

Soderling, T.R., and Derkach, V.A. (2000). Postsynaptic protein phosphorylation and LTP. Trends Neurosci. 23, 75-80.

Song, I., and Huganir, R.L. (2002). Regulation of AMPA receptors during synaptic plasticity. Trends Neurosci. 25, 578-588.

Strack, S., and Colbran, R.J. (1998). Autophosphorylation-dependent targeting of calcium/ calmodulin-dependent protein kinase II by the NR2B subunit of the N-methyl-D-aspartate receptor. J. Biol. Chem. 273, 20689-20692.

Tang, Y.P., Shimizu, E., Dube, G.R., Rampon, C., Kerchner, G.A., Zhuo, M., Liu, G., and Tsien, J.Z. (1999). Genetic enhancement of learning and memory in mice. Nature 401, 63-69.

Thiels, E., Barrionuevo, G., and Berger, T.W. (1994). Excitatory stimulation during postsynaptic inhibition induces long-term depression in hippocampus in vivo. J. Neurophysiol. 72, 3009-3016.

Tong, G., Shepherd, D., and Jahr, C.E. (1995). Synaptic desensitization of NMDA receptors by calcineurin. Science 267, 1510-1512.

Turner, D.A., Buhl, E.H., Hailer, N.P., and Nitsch, R. (1998). Morphological features of the entorhinal-hippocampal connection. Prog. Neurobiol. 55, 537-562.

Tzounopoulos, T., Kim, Y., Oertel, D., and Trussell, L.O. (2004). Cell-specific, spike timing-dependent plasticities in the dorsal cochlear nucleus. Nat. Neurosci. 7, 719-725.

Van Hoesen, G.W. (1995). Anatomy of the medial temporal lobe. Magn. Reson. Imaging 13, 1047-1055.

Watanabe, M., Mishina, M., and Inoue, Y. (1994). Distinct spatiotemporal expressions of five NMDA receptor channel subunit mRNAs in the cerebellum. J. Comp. Neurol. 343, 513-519.

Watanabe, S., Hoffman, D.A., Migliore, M., and Johnston, D. (2002). Dendritic K+ channels contribute to spike-timing dependent long-term potentiation in hippocampal pyramidal neurons. Proc. Natl. Acad. Sci. U. S. A. 99, 8366-8371.

Waters, J., and Helmchen, F. (2004). Boosting of action potential backpropagation by neocortical network activity in vivo. J. Neurosci. 24, 11127-11136.

Wenzel, A., Scheurer, L., Kunzi, R., Fritschy, J.M., Mohler, H., and Benke, D. (1995). Distribution of NMDA receptor subunit proteins NR2A, 2B, 2C and 2D in rat brain. Neuroreport 7, 45-48.

Yang, S.N., Tang, Y.G., and Zucker, R.S. (1999). Selective induction of LTP and LTD by postsynaptic [Ca2+]i elevation. J. Neurophysiol. 81, 781-787.

Yao, H., Shen, Y., and Dan, Y. (2004). Intracortical mechanism of stimulus-timing-dependent plasticity in visual cortical orientation tuning. Proc. Natl. Acad. Sci. U. S. A. 101, 5081-5086.

Yashiro, K., and Philpot, B.D. (2008). Regulation of NMDA receptor subunit expression and its implications for LTD, LTP, and metaplasticity. Neuropharmacology 55, 1081-1094.

Yeckel, M.F., and Berger, T.W. (1998). Spatial distribution of potentiated synapses in hippocampus: dependence on cellular mechanisms and network properties. J. Neurosci. 18, 438-450.

Yue, C., Remy, S., Su, H., Beck, H., and Yaari, Y. (2005). Proximal persistent Na+ channels drive spike afterdepolarizations and associated bursting in adult CA1 pyramidal cells. J. Neurosci. 25, 9704-9720.

Zhang, L.I., Tao, H.W., Holt, C.E., Harris, W.A., and Poo, M. (1998). A critical window for cooperation and competition among developing retinotectal synapses. Nature 395, 37-44.

Zhou, Q., Tao, H.W., and Poo, M.M. (2003). Reversal and stabilization of synaptic modifications in a developing visual system. Science 300, 1953-1957.

Zhou, Y., Takahashi, E., Li, W., Halt, A., Wiltgen, B., Ehninger, D., Li, G.D., Hell, J.W., Kennedy, M.B., and Silva, A.J. (2007). Interactions between the NR2B receptor and CaMKII modulate synaptic plasticity and spatial learning. J. Neurosci. 27, 13843-13853.